Title

The SidC and SidE families of Legionella pneumophila effectors differentially regulate ubiquitination, morphology, and stable capture of Rab5A at the bacterial vacuole surface

Permalink

Author

Steinbach, Adriana

Publication Date

2024

Peer reviewed|Thesis/dissertation

The SidC and SidE families of Legionella pneumophila effectors differentially regulate ubiquitination, morphology, and stable capture of Rab5A at the bacterial vacuole surface

by
Adriana Steinbach

DISSERTATION
Submitted in partial satisfaction of the requirements for degree of
DOCTOR OF PHILOSOPHY

in

Cell Biology

in the

GRADUATE DIVISION
of the
UNIVERSITY OF CALIFORNIA, SAN FRANCISCO

Approved:

Sophie Dumont
_____
Chair

Shaeri Mukherjee
_____

Mark von Zastrow
_____

Stephen Floor
_____

_____
Committee Members

ACKNOWLEDGEMENTS

I have worked in research labs on a variety of projects since I was sixteen years old, and I believed I knew what challenges lay ahead of me in grad school when I started at UCSF. I was wrong. This experience has been a humbling ultramarathon with intellectual, technical, and emotional hurdles that I had not remotely imagined, and I could not have done it without my support network of family, friends, and colleagues. Grad school can be very lonely at times – becoming an expert on a narrow slice of a field, experiencing the necessary struggle of piecing together hypotheses from ostensibly incoherent data – these are things that no one can help with directly. However, by providing emotional support, asking good questions, and wading a few feet into the swamp that I was up to my neck in, my scientific advisors and loved ones made an otherwise treacherous journey possible. It wasn't all bad, either, and these same people were there to celebrate successes as well. I cannot adequately express how grateful I am, but I will do my best.

First, to my immediate family – thank you for loving me unconditionally, and for buying me a lot of beer. You are all interesting, creative, and passionate people, and you inspire me every day. Dad - it has been so interesting to learn how to be a scientist with you. As a child, I thought your lab was one of the most beautiful and strange places I had ever seen, and it must have flipped some switch in my brain because I have sought out labs ever since. You have genuinely engaged with my science at every career stage, and your questions always get to the heart of the *why*, which is always the most interesting part. Thank you for staying curious, and for reminding me to do the same. Mom – thank you for teaching me to be tough, independent, and to value myself and my time. So many women (in science and otherwise) burn out trying to please and help others before taking care of themselves, and you always reminded me not to sacrifice myself for those who don't deserve it. I have come to appreciate your example and encouragement even more through the experience of grad school. Thank you for reminding me to have fun, and for

– you bring us so much joy every day, both by being a wonderful human and by pronouncing about five percent of the words you say like an absolute madwoman. Chetan – you've worked with me at my maximal stress and chaos levels in the short time you've been in the lab, and still have done so well (although your vernacular could use some expansion). We are all proud of you both! Finally, thank you to Daryll Gempis for keeping the Hooper running; we would not get anything done without you.

I have had many notable scientific mentors outside of Shaeri's lab. Thank you to my thesis committee: Sophie Dumont, Mark von Zastrow, and Stephen Floor. In meetings, you asked questions that pushed my science forward, and I always felt like you were advocating for me as a scientist and as a person. I appreciate your candidness in conversations about careers and your experiences in academia. Sophie talked me through my lowest point in grad school and helped me realize that I hadn't ruined everything beyond saving. I am grateful to have had the support of a group of scientists that I respect so much. Thank you to Erin Adams, my PI as an undergrad and technician at the University of Chicago, for setting the bar astronomically high for mentorship and excellence in research. Charlie Dulberger, my direct supervisor in Erin's lab, taught me so much about doing science, and also not to take things quite so seriously all the time. I have relied on the skills I learned from both Erin and Charlie throughout my time in grad school, and I cannot thank them enough for their mentorship. Thank you to Meghan Morrissey, my mentor during my rotation in Ron Vale's lab, for teaching me how to use fancy microscopes and encouraging me to prioritize the "life" part of "work-life" balance.

The main reason I chose Tetrad rather than any other grad program was because I felt like the students I met at UCSF were my people, and that has absolutely proved to be the case. My class is chock full of interesting, brilliant, and thoughtful people. Francesca Del Frate and I became instant friends, and living together for the past five years has brought so much joy, cathartic yelling, and yarn into my life. Dana Kennedy and Elise Muñoz are as kind as they are kickass scientists; thank you for helping me feel my feelings and always bringing the party. Chris

CONTRIBUTIONS

Chapter 2 includes materials previously published in Molecular Biology of the Cell. Varun Bhadkamkar, co-first author on this publication, carried out many experiments on Rab1 and Rab10 recruitment and ubiquitination during *Legionella* infection that inform the models that I propose for Rab5. He found that Rab1 must be recruited to the bacterial vacuole to be ubiquitinated, and, as I observe for Rab5, that the SidE family of effectors is required for Rab1 polyubiquitination. Additionally, Varun did a huge amount of analysis of the proteomic data and was the first to notice the ubiquitination of small GTPases across the Ras superfamily during infection. He was easily my closest collaborator on this work and contributed intellectually to the models proposed in the Chapter 2 Discussion and to the crosslinking hypothesis proposed in the Chapter 3 Discussion. The schematic of the experimental setup for the proteomic analysis in Figure 2.2 was created by Julia Noack.

Steinbach, A.*, Bhadkamkar, V.*, Jimenez-Morales, D., Stevenson, E., Jang, G.M., Krogan, N.J., Swaney, D.L., and Mukherjee, S. (2024). Cross-family small GTPase ubiquitination by the intracellular pathogen Legionella pneumophila. Mol. Biol. Cell *35*, ar27. 10.1091/mbc.e23-06-0260.

*co-first authors

Materials in Chapter 3 are included in a manuscript currently in preparation.

The SidC and SidE families of *Legionella pneumophila* effectors differentially regulate ubiquitination, morphology, and stable capture of Rab5A at the bacterial vacuole surface

Adriana Steinbach

ABSTRACT

Intracellular bacterial pathogens have evolved to survive in a distinctly hostile environment. Intravacuolar pathogens such as *Legionella pneumophila* (*L.p.*) reside within a membrane-bound compartment in their host cell, reshaping host materials into a new, protected organelle. The molecular mechanisms employed by *L.p.* during early infection to defend its vacuole are not entirely understood. As host cells uptake the bacterium by phagocytosis, *L.p.* must avoid classical trafficking of its phagosome through the endolysosomal pathway and attack by autophagy, which would ultimately lead to destruction of the bacterium in the lysosome. In this work, we set out to define how *L.p.* manipulates host regulatory proteins to defend its vacuole, termed the *Legionella*-containing vacuole (LCV), from these threats during early infection. First, we explore the interaction of the host small GTPase Rab5 with the LCV. Rab5 is the master regulator of the early endosomal compartment and is required for phagosome maturation. We determine that Rab5 associates with the LCV and is both mono- and polyubiquitinated during infection. This ubiquitination is dependent on two groups of secreted bacterial effector proteins: SidC/SdcA and the SidE family. SidC/SdcA are required for both mono- and polyubiquitination of Rab5, whereas the SidE family is largely responsible for polyubiquitination. We find that SidE family-dependent polyubiquitination is necessary for retention of Rab5 at the LCV membrane. Next, we recognized that Rab5 presents a unique experimental opportunity to study how host proteins are modified by effectors at the LCV, as Rab5 localizes to both the WT and avirulent

strain LCV. We determine that Rab5 associated with the WT LCV has exceptionally high stability and a distinctive morphology dependent on the SidE family of effectors rather than host regulators. Finally, we discover that *L.p.* infection induces a burst of ubiquitination of both host and bacterial proteins and that SidC/SdcA are likely required for this burst. We propose a new role for SidC/SdcA as metaeffectors, regulating the activity of other as yet unknown bacterial proteins. Taken together, our findings suggest a model in which *L.p.* uses ubiquitin as a tool to retain and stabilize proteins at the LCV membrane, perhaps playing a role in containment of deleterious host proteins or participating in a physical blockade around the vacuole. This work illustrates the complex interplay between two fascinating families of *L.p.* effectors and refines our understanding of the strategies utilized by *L.p* to protect its vacuole during early infection.

TABLE OF CONTENTS

LIST OF FIGURES

LIST OF TABLES

LIST OF ABBREVIATIONS

CTCF	Corrected total cell fluorescence
CTLF	Corrected total LCV fluorescence
diGly	Diglycine
DUB	Deubiquitinase, deubiquitinating enzyme
EEA1	Early endosome antigen-1
ER	Endoplasmic reticulum
FcγR	Fc-gamma receptor
GAP	GTPase activating protein
GDP	Guanosine-5'-diphosphate
GEF	Guanine nucleotide exchange factor
GTP	Guanosine-5'-triphosphate
hpi	Hours post-infection
L.p.	*Legionella pneumophila*
LCV	*Legionella*-containing vacuole
Log2FC	Log_2(Fold Change)
MOI	Magnitude of infection
PI(3)P	Phosphatidylinositol 3-phosphate
$PI(3,5)P_2$	Phosphatidylinositol 3,5-bisphosphate
PI(4)P	Phosphatidylinositol 4-phosphate
PtdIns	Phosphoinositides
PTM	Post-translational modification
PR-ubiquitination	Phosphoribosyl ubiquitination
T4SS	Type IV secretion system
WT	Wildtype

CHAPTER 1 : INTRODUCTION

Legionella pneumophila Controls Membrane Trafficking in Diverse Eukaryotic Hosts

To survive and replicate, intracellular pathogens must reconfigure host cells to acquire resources for growth while also avoiding detection and destruction by host cell defenses. For pathogens internalized via endocytosis or phagocytosis, the first obstacle presented by the host cell is the endolysosomal system. Internalized cargo enclosed in endocytic vesicles is sorted and directed to the appropriate compartment, and endosomes containing material destined for destruction mature and eventually fuse with lysosomes, low pH vesicles containing enzymes that degrade biological macromolecules[1]. Bacterial pathogens that rely on endocytic uptake to infect host cells have evolved a range of strategies to avoid degradation in the lysosome. Some pathogens, such as *Listeria monocytogenes,* disrupt the phagosome membrane and escape into the host cell cytoplasm[2]. Others, such as *Coxiella burnetii,* allow phagosome maturation and sense the low pH of the lysosome to initiate the release of virulence factors[3]. *Legionella pneumophila* (*L.p.*), a facultative intracellular bacterial pathogen, has a less well-defined relationship with the endo-lysosomal compartment. The bacterium is internalized by host cells via phagocytosis and resides within a phagosome-derived compartment throughout its life cycle in the host cell, unlike *Listeria*[4], and yet this vacuole resists fusion with the lysosome throughout early infection, unlike *Coxiella*[5]. While this phenotype is not unique to *L.p.*, the molecular mechanisms that protect the membrane-bound compartment enclosing the bacterium, known as the Legionella-containing vacuole (LCV), during the early infection stages are poorly understood.

In the decades since the discovery of *L.p.*, it has become clear that bacterial proteins injected into the host cell cytosol, called effector proteins or simply effectors, are required for bacterial survival[6]. Once internalized, *L.p.* uses a Type IV secretion system (T4SS), a protein translocation channel that spans both the bacterial and LCV membranes, to transfer ~330

effectors into the host cell. The activity of these effector proteins subverts host membrane trafficking to mediate dynamic contacts between the LCV and endoplasmic reticulum (ER)-derived vesicles, smooth ER tubules, and to eventually transform the LCV into a rough ER-like organelle[7,8]. While most effectors have undefined functions, those that have been characterized modulate diverse host processes such as autophagy[9], gene expression[10], and protein translation[11–13]. *L.p.*'s enormous arsenal of effectors has been hypothesized to permit its unusually wide range of permissive host cells[14]. While *L.p.* can infect alveolar macrophages in immunocompromised humans causing a severe pneumonia known as Legionnaires' disease, its preferred hosts include a diversity of freshwater protozoa. Cell biologists have long been intrigued by this bacterial pathogen due to its evolutionarily divergent range of host cells, as it suggests *L.p.* manipulates fundamentally conserved eukaryotic cell biological processes. In all infection contexts, disruption of effector secretion by genomic deletion of T4SS components results in an avirulent strain of *L.p.* that is efficiently trafficked to the lysosome[15]. Notably, not only do very few single effector knockout strains have growth defects, but deletion of over 20% of *L.p.*'s effector arsenal still permits intracellular replication in macrophages[16], suggesting that *L.p.*'s defense mechanisms during early infection are robust and likely redundant.

Endosome Maturation

Eukaryotic cells internalize and direct material from the extracellular environment through a dynamic network of vesicular organelles known as the endolysosomal system. The endolysosomal system carries out diverse roles in the cell, from signaling and nutrient acquisition to the destruction of invading pathogens[17]. To avoid trafficking to the lysosome, *L.p.* must manipulate or dodge the process of endosome maturation. Normal progression through the endolysosomal pathway is a complex, dynamic process that requires continuous re-shaping of vesicle membrane identity generated both by enzymatic activity as well as highly regulated fusion and fission events. Phagosomes, generated by the specialized endocytic process of

phagocytosis, are plasma membrane-derived vesicles formed upon internalization of bulky extracellular material. While phagocytosis requires specialized signaling at the plasma membrane throughout the uptake process, after internalization the protein components involved in maturation are largely shared with the endosomal system[18]. Shortly after formation, these nascent membrane-bound compartments immediately undergo extensive remodeling of protein and lipid components of the cytosolic leaflet, mediated in large part by a series of Rab proteins, small GTPases in the Ras superfamily that play a pivotal role in membrane identity specification in eukaryotic cells. All Rab proteins share a similar bimodal activity cycle: an active, membrane associated, GTP-bound state that permits conformation-specific interaction with GTPase-specific binding partners, and an inactive, cytosolic, GDP-bound state. This activity cycle is highly regulated - GDP release is mediated by guanine nucleotide exchange factors (GEFs), and GTPase activity and subsequent inactivation is stimulated by GTPase activating proteins (GAPs)[19]. Rab5 is activated at early endosomal membranes and recruits binding partners that mediate fusion between early endosomal compartments and cargo sorting. The switch from Rab5 to Rab7 on the endosome membrane mediates the transition from early to late endosome and is required for eventual fusion with the lysosome[1]. This Rab switch is coordinated by the Mon1-Ccz1 complex, the Rab7 GEF, which binds both the Rab5 GEF Rabex5[20] and the phosphoinositide PI(3)P (discussed below)[21]. In addition to activating Rab7, Mon1-Ccz1 displaces Rabex5, preventing further activation of Rab5 at the endosomal membrane[20].

Rab5 and Rab7 binding partners also mediate a switch in membrane phosphoinositide (PtdIns) composition. PtdIns are low-abundance membrane phospholipids that participate in signaling and compartment identity specification in all eukaryotic cells. The polar head group of the lipid is an inositol ring with three free hydroxyl groups at positions 3-5 accessible to cytosolic lipid kinases, and the position(s) of head group phosphorylation determines the species of PtdIns[22]. Many proteins are anchored to target membranes at least in part through specific PtdIns binding domains that recognize these phosphorylation patterns on the inositol ring. Early

endosomes are characteristically PI(3)P-positive due to the activity of the Rab5-GTP binding partner hVps34, a lipid kinase. During Rab7 displacement of Rab5, PIKFYVE, a lipid kinase that recognizes PI(3)P, shifts the membrane composition towards PI(3,5)P$_2$[18]. As the membrane lipid composition shifts and Rab7 and its binding partners supplant Rab5, the endosomal compartment acidifies and becomes competent for fusion with lysosomes, resulting in the degradation of cargo destined for destruction.

Legionella and the Endolysosomal System

Work from several groups has determined that the WT LCV does not undergo typical endosome maturation. While there is evidence that the LCV eventually acidifies and fuses with lysosomes at very late stages of infection (16+ hours), in the pre-replicative stage *L.p.* avoids the process of endosome maturation[23]. The PtdIns composition of the vacuole membrane surrounding *L.p.* WT shifts from PI(3)P during early infection to PI(4)P, rather than PI(3,5)P$_2$, through the coordinated action of multiple effectors. On the other hand, the membrane surrounding *L.p.* $\Delta dotA$ remains PI(3)P positive throughout early infection[24]. No single or combinatorial bacterial effector knockout strain has been generated that completely prevents the accumulation of PI(4)P at the membrane[25], so it is unknown whether the PI(3)P to PI(4)P switch is required for lysosome fusion evasion during infection. However, it is clear that this PtdIns switch is important for bacterial pathogenesis as multiple *L.p.* effectors are anchored to the LCV membrane by binding PI(4)P[26,27].

The extent of association of endosomal Rab proteins with the WT LCV is less well established. Early studies suggested that Rab5, but not Rab7, was excluded from the WT LCV[28,29], but more recent work has suggested that both endosomal small GTPases are associated with the WT LCV in macrophage-like cells at one hour post-infection (hpi)[30]. Several bacterial effectors have been found to interact with Rab5, suggesting that *L.p.* may face survival pressure to modulate Rab5. One, VipD, is a phospholipase that is activated upon binding Rab5-GTP, and,

when ectopically expressed, reduces endosomal localization of the PI(3)P biosensor GFP-FYVE[31]. The authors propose that VipD acts on endosomes adjacent to the LCV during infection, depleting PI(3)P. This would likely inhibit homotypic fusion given that EEA1, which is required for fusion, is anchored to endosomal membranes in part by PI(3)P[32], and that membrane lipid composition affects the efficiency of SNARE based fusion[33]. Accordingly, previous work has demonstrated that the WT LCV is resistant to fusion with early endosomes[34]. Another *L.p.* effector, lpg0393, shows *in vitro* GEF activity towards Rab5, and has some structural similarity to the eukaryotic Rab5 GEF Rabex5[35]. However, the authors find that ectopically expressed lpg0393 localizes to the Golgi and provide no experimental results on the role lpg0393 may play in infection, so it remains unclear how this effector may modulate Rab5 activity during *L.p.*'s life cycle.

Another consideration in investigating how *L.p.* evades the host endolysosomal system is scale - if *L.p.* is inhibiting host regulatory proteins during infection, is this inhibition A) limited to the LCV membrane, B) affecting the LCV and nearby organelles as proposed for VipD[31], or C) globally applied across the host cell? There are several lines of evidence that *L.p.* effectors predominantly exert their protective effect at or near the LCV membrane. First, macrophages infected with *L.p.* and challenged with heat killed yeast at various time points across early infection efficiently traffic the yeast cells to the lysosome[36]. Furthermore, two studies have carried out co-infection experiments with WT *L.p.*, one with an avirulent strain of *L.p.*[36], and another with an avirulent mutant strain of the intracellular pathogen *Brucella neotomae*[37]. In both cases it was found that only the avirulent bacteria within the same phagosome as WT *L.p.* were able to replicate during coinfection. These findings suggest that the inhibition of lysosomal fusion enforced by *L.p.* effectors is likely limited to the LCV membrane and does not extend globally throughout the host cell.

Ubiquitin

A central element of *L.p.* pathogenesis, signaling within the endolysosomal system, and host defenses against invading bacteria is the ubiquitin signaling network. Ubiquitin is a small, highly conserved globular protein used by eukaryotic cells as a post-translational modification (PTM). Ubiquitin is conjugated to target proteins via a covalent bond between the C-terminus of the ubiquitin molecule and a labile amine, thiol, or hydroxyl group[38] on the target protein, most frequently a lysine side chain amine. Canonically, eukaryotic cells attach ubiquitin to a substrate protein using ATP and the sequential activity of ubiquitin-activating (E1), ubiquitin-conjugating (E2), and ubiquitin ligase (E3) enzymes. Ubiquitination is reversible; ubiquitin can be removed from target proteins by deubiquitinating enzymes (DUBs). The addition of a single ubiquitin molecule to a target protein is monoubiquitination, and the attachment of single ubiquitin molecules on multiple target protein sites, multi-monoubiquitination. Ubiquitin itself has seven lysine residues onto which additional ubiquitin molecules can be conjugated, resulting in polyubiquitin chains. Mono, multi-mono, and polyubiquitination events have distinct signaling outcomes in the eukaryotic cell, which can be even more complex in the case of polyubiquitination, as the identity of the particular lysine residue linked to the next ubiquitin molecule in the chain determines downstream recognition and processing[39]. Ubiquitin signaling regulates a huge diversity of eukaryotic cell biological processes, but most relevant to this study include the ubiquitination of cell surface receptors to induce endocytic uptake and trafficking to the lysosome[40], and the targeting of pathogen vacuoles with ubiquitin chains to initiate immune signaling and autophagy[41,42].

Perhaps in part as a response to host ubiquitin-based defenses, almost 30 translocated *L.p.* effectors to date have been characterized to possess either ubiquitin ligase or DUB activity[43]. These include the paralogous ligases SidC and SdcA, which promote the recruitment of as yet unknown ubiquitinated substrates and ER-membranes to the LCV[44–46]. SidC/SdcA also play a

role in the ubiquitination of two small GTPases important for *L.p.* pathogenesis, Rab1 and Rab10, although how SidC/SdcA are involved and the consequences of ubiquitination on Rab1/10 are not yet known[47,48]. The repertoire of secreted ubiquitin ligases also includes the SidE family (SidE, SdeA, SdeB, SdeC), which catalyze non-canonical phosphoribosyl-ubiquitination (PR-ubiquitination), entirely bypassing the host E1-E2-E3 cascade and thwarting host DUBs[49,50]. A growing list of *L.p.* DUB effectors that act on canonically ubiquitinated substrates includes LotC/Lem27, which may regulate the deubiquitination and recruitment of Rab10[51]. The tight relationship between *L.p.* pathogenesis and ubiquitin has been further demonstrated by studies connecting host ubiquitin pathways to efficient translocation of effectors through the T4SS[52], ubiquitin binding to the activation of the effector VpdC involved in vacuolar expansion[53], and effector secretion to the suppression of ubiquitin-rich DALIS structures involved in antigen presentation by immune cells[54].

The Vacuole Guard Hypothesis

While endosome maturation and recognition by autophagy machinery are often (even in this introduction) described as acute threats to intravacuolar bacterial pathogens, the reality must be somewhat more complicated. *L.p.*'s intracellular life cycle lasts for about 16-24 hours[23], and the LCV is under constant threat from host cell defenses. A growing movement in the host-pathogen field has recognized that intravacuolar pathogens must continually maintain the integrity of their surrounding membrane throughout infection, and the effectors that carry out this function have been termed "vacuole guards"[55]. For example, *Salmonella* Typhimurium, usually an intravacuolar pathogen, is released into the cytoplasm when lacking its effector SifA, and subsequently fails to replicate[56]. Several *L.p.* effectors have been proposed to act as vacuole guards, the best characterized being SdhA, which binds the host PI-phosphatase OCRL to prevent fusion of the LCV with endocytic vesicles[57]. Much like the *sifA* mutant *S.* Typhimurium strain, the ∆*sdhA* strain is exposed to the host cell cytoplasm and has a replication defect without

an increase in trafficking to the lysosome[58]. More recently, the SidE family of non-canonical ubiquitin ligases have been implicated as vacuole guards, potentially by creating a physical barrier of PR-ubiquitinated ER-tubules[59], and by masking ubiquitin chains surrounding the LCV to prevent recognition by autophagy machinery[60].

Project Objective and Findings

This study's broad goal is to define the molecular mechanisms by which *L.p.* protects the LCV from the host cell during early infection. Initially, we focus on the early endosome regulators that *L.p.*'s vacuole was likely to encounter shortly after formation, most notably Rab5. We find that Rab5 associates with both the WT and Δ*dotA* LCV, but localizes to the WT LCV membrane throughout early infection, whereas the Δ*dotA* LCV loses Rab5 association after the first hour after internalization. We find that Rab5 is differentially mono- and polyubiquitinated in a manner dependent on both the SidC and SidE families of *L.p.* effectors, respectively, and that polyubiquitination stabilizes Rab5 in membranes. Notably, both families of effectors are required for LCV localization of Rab5. This finding is somewhat puzzling, as Rab5 is thought to be an antagonist of the *L.p.* lifecycle, so we explored the hypothesis that ubiquitinated Rab5 may be incorporated into a protective barrier around the LCV. Our experiments indicate that WT LCV-associated Rab5 is exceptionally stable and exhibits an unusual, "cloud"-like morphology, and that this morphology is dependent on the SidE family of effectors. These findings are consistent with Rab5 incorporation into a ubiquitin "shield", a barrier which has been proposed to act as vacuole guard[59,60]. Finally, given the central role that ubiquitin plays in *L.p.* pathogenesis coupled with the findings from our lab and others that *L.p.* may use ubiquitin as a tool to protect its vacuole, we focus more broadly on ubiquitination events specific to *L.p.* WT infection. We find that a burst of ubiquitination of both host and bacterial proteins occurs during the first hour of infection, and that the SidC effectors are required for this burst. As SidC effectors are also required for the accumulation of the coat of ubiquitinated proteins that surround the WT LCV shortly after

formation[47], we were particularly intrigued by this finding. However, as SidC/SdcA have no known host or bacterial targets of their ubiquitin ligase activity, we propose an alternative mechanism of action for these mysterious effectors, wherein they may act as metaeffectors, regulating the activity of other bacterial effectors during infection. Overall, our findings reveal a complex interplay between two key families of bacterial effectors in manipulating the host ubiquitin system to control host proteins and protect the LCV.

CHAPTER 2 : MULTI-STEP EFFECTOR-DRIVEN RAB5 UBIQUITINATION CONTROLS LCV ASSOCIATION

Introduction

Rab5 is the master regulator of the early endosomal compartment in eukaryotic cells and required for endosome maturation[17]. To clarify how *L.p.* protects its vacuole from the endolysosomal system during early infection, we initially focus on Rab5 interactions with the LCV. We find that Rab5 does in fact localize to the WT LCV during early infection, but, surprisingly, with a higher frequency across early infection than observed for the avirulent Δ*dotA* strain. Rab5 recruitment to the WT LCV does not result in association of early endosome marker EEA1, indicating that Rab5 does not generate an early endosome-like character at the WT LCV membrane. We determine that Rab5 is targeted with both mono- and polyubiquitination during *L.p.* infection, and that this ubiquitination is likely non-degradative. We find that membrane association of Rab5 is required for ubiquitination, and that effectors SidC and SdcA are necessary, but not sufficient, for the ubiquitination of Rab5. Intriguingly, SidC/SdcA are also required for Rab5 recruitment to the LCV, suggesting a complex interplay between SidC/SdcA activity, Rab5 membrane association, and ubiquitination. Finally, we determine that effectors in the SidE family function downstream of SidC/SdcA to promote Rab5 poly-ubiquitination, which retains it in the LCV membrane. Altogether, our data suggest that *L.p.* modulates Rab5 during infection through the concerted activity of several effectors, resulting in a distinctively stable association with the LCV membrane.

Rab5 Associates with the LCV Throughout Early Infection

To determine whether Rab5 is excluded from the LCV membrane by bacterial effectors during *L.p.* infection, we carried out immunofluorescence analysis of endogenous Rab5A in
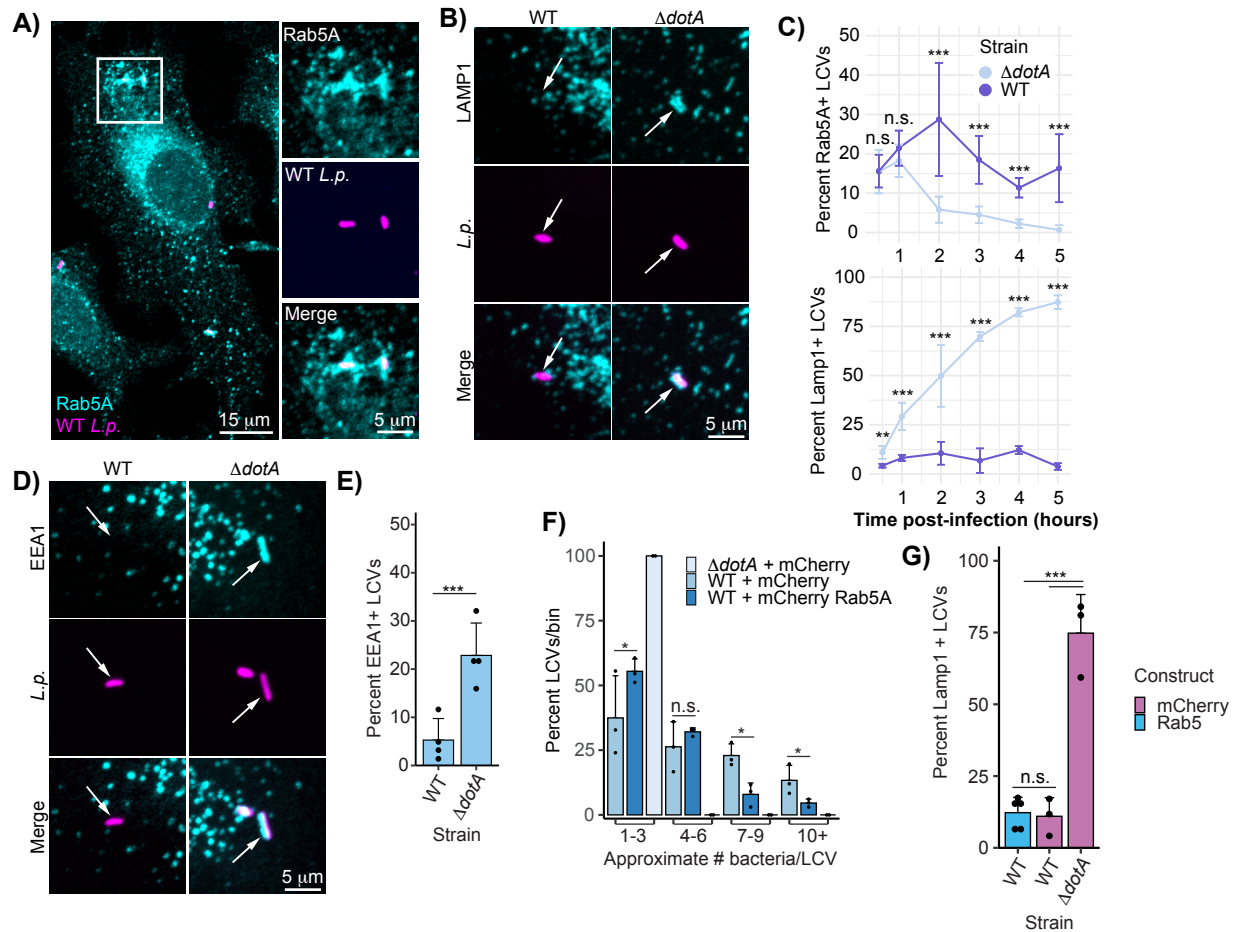
Figure 2.1 Rab5 associates with the WT LCV.

Representative images of **(A)** WT LCV Rab5A recruitment (1hpi), and **(B)** Lamp1 exclusion from the WT LCV (4hpi). **(C)** Quantification Lamp1 and Rab5 recruitment – percent of LCVs per biological replicate positive for indicated marker (n=3, 75-150 LCVs scored per replicate, adj. pvalue = 0.08). **(D)** EEA1 associates with the Δ*dotA* but not WT LCV. HeLa FcγR cells were infected with *L.p.* WT or Δ*dotA* (MOI=1) for 1 hour, fixed, and probed with anti-EEA1 and anti-*Legionella* antibodies. **(E)** Quantification of EEA1 recruitment as in (C); n=4, 75-150 LCVs scored per replicate, p value = 0.05. **(F)** *L.p.* replication is inhibited by Rab5A overexpression. HeLa FcγR cells were transfected with mCherry tagged Rab5A or mCherry alone, infected with WT or Δ*dotA* for 10 hours, fixed, and probed with anti-*Legionella* antibodies. Bacteria count per LCV was approximated by measuring the LCV area and dividing by the average area of the Δ*dotA* LCVs. For each biological replicate (n=3, 25-50 LCVs per replicate, adj. p-value = 0.013), we tabulated the number of LCVs falling into the indicated bin and calculated the percent each bin represented of the total. **(G)** Rab5 overexpression does not increase frequency of WT LCV Lamp1 staining. HeLa FcγR cells transfected with mCherry Rab5A or mCherry alone were infected with *L.p.* WT or Δ*dotA* for 4 hours, fixed, and probed with anti-Lamp1 and anti-*Legionella* antibodies. For each biological replicate, the percent of LCVs scored positive for the indicated marker was calculated (n=3-4, 75-150 LCVs scored per replicate, adj. p-value = 0.017)

HeLa FcγR cells infected with *L.p.* WT or Δ*dotA* across a time range from 30 minutes to 5hpi. We observed clear Rab5A recruitment to both the WT and Δ*dotA* LCV, while the WT LCV still resists lysosomal fusion, as shown by the exclusion of the lysosomal membrane protein Lamp1 (**Fig 2.1A-B**). Interestingly, whereas the Δ*dotA* LCV shows more canonical Rab5A dynamics in which recruitment peaks shortly after internalization and decays quickly thereafter, the WT LCV shows moderate frequencies of Rab5A localization across the first five hours of infection **(Fig2.1C)**.

We next assessed whether localization of Rab5 to the LCV results in the accumulation of early endosomal markers. Rab5A-GTP recruits early endosome-specific proteins both through direct binding interactions and by the production of the phosphoinositide PI(3)P via the activity of multiple binding partners[61]. One such protein is early endosome antigen 1 (EEA1), which binds to both Rab5-GTP and PI(3)P[32,62]. Despite Rab5 association with the WT LCV, we do not observe recruitment of EEA1 at 1hpi, while EEA1 robustly localizes to the Δ*dotA* LCV (**Fig 2.1D-E**). Notably, multiple *L.p.* effectors are known to coordinate the conversion of PI(3)P to PI(4)P at the LCV membrane during early infection[26,63], and the exclusion of EEA1 suggests that this lipid conversion program is active even while Rab5A is present. Conversely, association of Rab5A with the WT LCV is not sufficient to promote an early endosome-like character at the membrane, in contrast to the Δ*dotA* LCV. To determine if Rab5A activity is detrimental to *L.p.*, we assayed both bacterial replication and lysosomal trafficking of the LCV in the context of Rab5 overexpression. HeLa FcγR transfected with mCherry-Rab5A or mCherry alone were infected with *L.p.* WT or Δ*dotA*, fixed at 4 and 10hpi, and subjected to immunofluorescence analysis. At 10hpi, there is a small but significant decrease in the frequency of high bacterial burden LCVs during Rab5A overexpression compared to control (**Fig 2.1F**). However, there is no increase in Lamp1 positive WT LCVs at 4hpi during Rab5A overexpression (**Fig 2.1G**), further suggesting

that Rab5 recruitment and activity does not promote trafficking of the WT LCV through the endolysosomal pathway.

Rab5 is Mono- and Polyubiquitinated During *L.p.* Infection

The clear differences in both Rab5 LCV association dynamics and the recruitment of early endosome and lysosome markers between *L.p.* WT and Δ*dotA* suggest that bacterial effectors modify the function of Rab5 during infection. A common strategy employed by pathogens to subvert host protein function is to post-translationally modify these proteins, either directly through the activity of effectors, or indirectly by manipulating the host's own regulatory network. *L.p.* is known to extensively modify proteins by ubiquitination during infection and has been previously shown to ubiquitinate small GTPases in the Rab family[47,48]. To understand changing patterns of ubiquitination during *L.p.* infection, we performed a global proteomics analysis of protein ubiquitination changes in *L.p.*-infected cells. We chose HEK293 cells stably expressing the FcγRIIb receptor (HEK293 FcγR cells), as HEK293 FcγR have been used extensively in previous studies of *L.p.* pathogenesis and efficiently internalize antibody-opsonized *L.p.*[13,50,64–66]. Cells were left uninfected or infected with either *L.p.* WT or the non-pathogenic *L.p.* Δ*dotA* strain (**Fig 2.2A**). For temporal resolution, infected cells were lysed at 1- or 8-hours post-infection (hpi). Extracted proteins from these five conditions (uninfected control, WT 1hr, WT 8hr, Δ*dotA* 1hr, Δ*dotA* 8hr) were trypsinized and processed with diGlycine (diGly) remnant enrichment, which is found upon protein modification with ubiquitin. While diGly enrichment also captures peptides modified with the ubiquitin-like proteins NEDD8 and ISG15, these peptides make up only a small fraction of the total enriched pool (~5%)[67]. It is important to note that this enrichment strategy can identify only canonically ubiquitinated sites; PR-ubiquitination mediated by the SidE family will not be detected. Enriched peptides were then subjected to mass spectrometric analysis and quantified with appropriate adjustments made based on quality control metrics (see Materials and
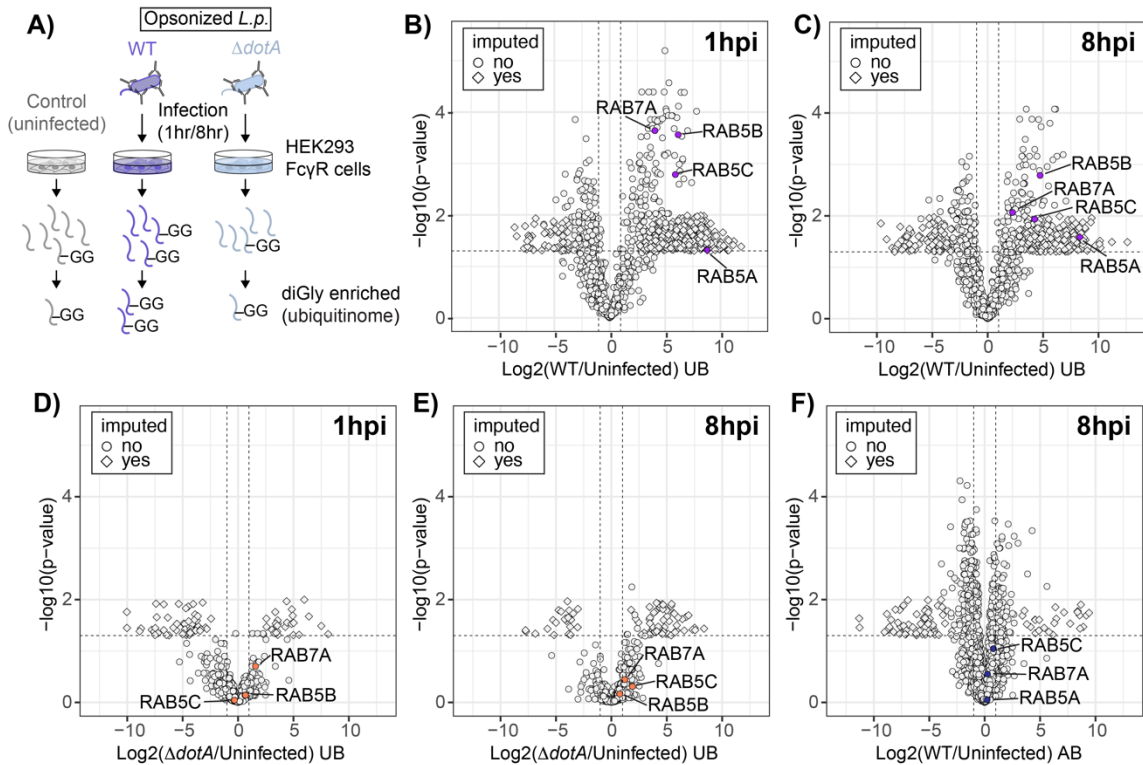
Figure 2.2 Endosomal Rabs are ubiquitinated during *L.p.* infection.

(A) Schematic of sample preparation for proteomic analysis. **(B)**-**(C)** Volcano plots representing ubiquitinomics and abundance data for indicated conditions.

Methods). As ubiquitination of target proteins can result in proteasomal degradation[39], we compared host cell protein ubiquitin changes to changes in abundance. To do this, we analyzed our pre-diGly enriched cell lysates via mass spectrometry and quantitated changes in host protein abundance. For detailed quality control analysis, complete information about instrument settings during data acquisition, and a full summary of pathway and protein complex analysis, we refer the reader to our recent publication in Molecular Biology of the Cell[68].

We next determined how ubiquitination changes for individual proteins between the different conditions. We calculated the Log2 fold changes (Log2FC), corresponding p-values, and adjusted p-values for all detected proteins across all pairwise combinations of conditions (uninfected, WT and Δ*dotA* infected). Unsurprisingly, we encountered many instances in which a peptide was uniquely detected in one of the conditions while missed in the other one (e.g., a novel

14

protein ubiquitination detected in WT infected but not uninfected control cells). Log2FC and

adjusted p-values were calculated for these events using a suitable imputation strategy in which

the missing peptide intensity value was assigned from the threshold of detection (see Methods).

In our subsequent analyses, we focused on four comparisons: WT1hr-Control, WT8hr-Control,

ΔdotA1hr-Control, and ΔdotA8hr-Control (hereafter referred to as WT1hr, WT8hr, ΔdotA1hr, and

ΔdotA8hr). Significant ubiquitination was determined using joint thresholds of |Log2FC| ≥ 1, adj.-

p-value < 0.05]. Our unbiased mass spectrometry analysis reveals that all three genetically

encoded Rab5 isoforms (RAB5ABC) and late endosomal regulator Rab7A are ubiquitinated

during *L.p.* WT, but not Δ*dotA*, infection (**Fig 2.2 B-E**). Notably, none of the endosomal Rabs

detected show a significant decrease in abundance at 8 hpi during WT infection, suggesting that

in this case, *L.p.* effector-induced Rab ubiquitination is not primarily degradative **(Fig 2.2F)**.

The diGly enrichment strategy used in the proteomic analysis isolates canonically

ubiquitinated peptides by recognizing the two glycine remnant at the ubiquitin attachment site on

the target protein after tryptic digest, and thus provides no information about mono- vs

polyubiquitination, or polyubiquitin chain composition. To roughly assess patterns of Rab5

ubiquitination induced by *L.p.* effectors, we infected U937 macrophage-like cells for 1, 2, 4, and

6 hours, and assayed Rab5 mass shifts by Western blotting. We observed the accumulation of

an approximately 8.5 kDa upshifted species at all timepoints during *L.p.* WT, but not Δ*dotA*,

infection, corresponding to the addition of a single ubiquitin molecule (**Fig 2.3A**). This WT infection

induced mass shifted species is also observed for endogenous Rab5A in HEK293T FcγR, as well

as Flag-tagged Rab5B and C in HEK293T FcγR (**Fig 2.3B-C**). To confirm that this higher

molecular weight species is monoubiquitinated Rab5A, we immunopurified Flag-Rab5A from

HEK293T FcγR cells co-expressing low levels of HA-ubiquitin (see Methods) and infected with

L.p. WT or Δ*dotA.* In WT infected, but not Δ*dotA* infected or uninfected pulldown samples,
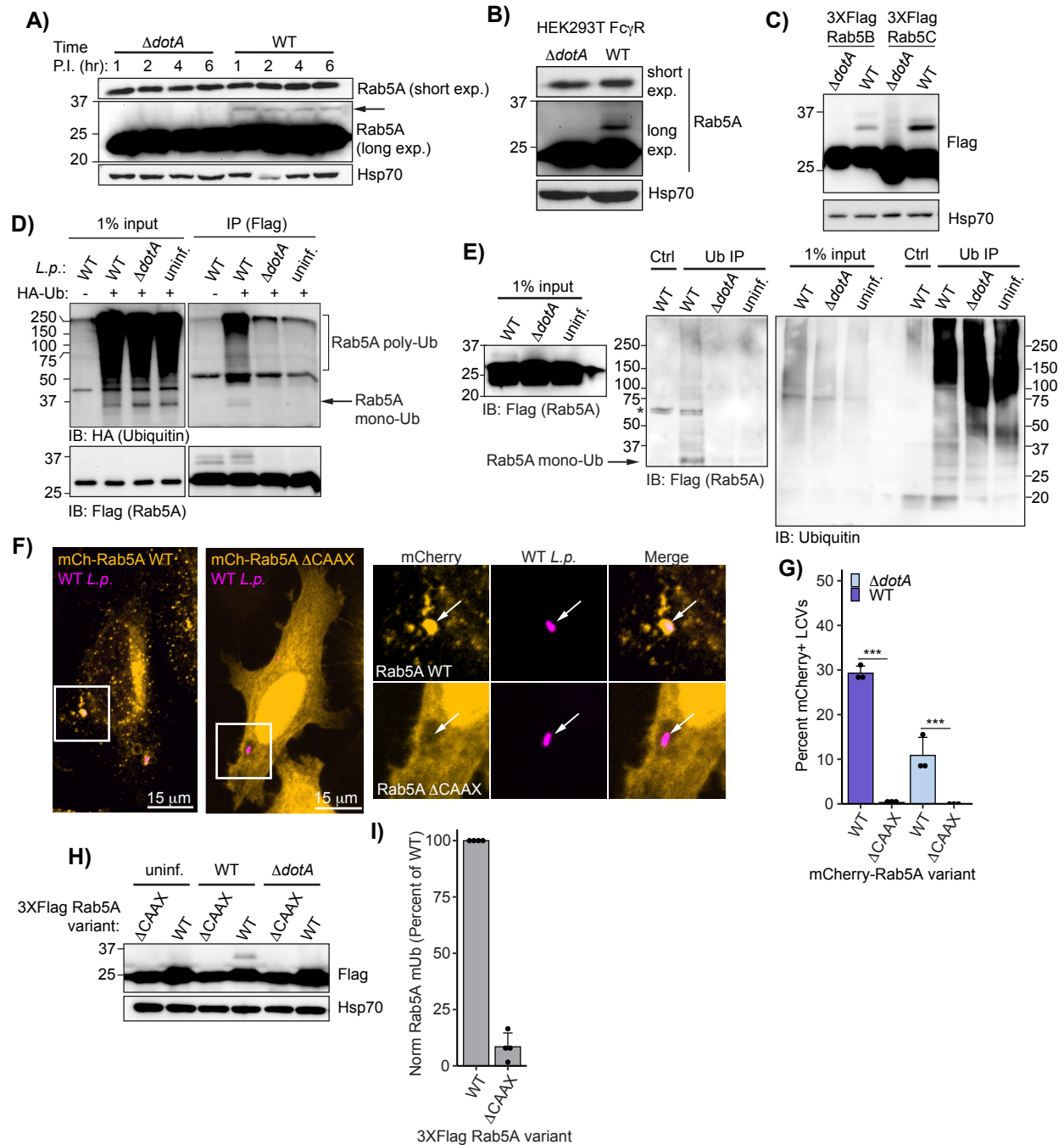
Figure 2.3 Rab5 is mono- and polyubiquitinated during *L.p.* infection.

(A) Immunoblot analysis of endogenous Rab5A mass shift during *L.p.* WT or Δ*dotA* infection. U937 cells differentiated into macrophage-like cells were infected with either WT or Δ*dotA* (MOI = 50) and lysed at the indicated time point. **B)** Immunoblot analysis of endogenous Rab5A in lysates prepared from HEK293T FcγR and infected with *L.p.* WT or Δ*dotA* (MOI = 20). **(C)** Immunoblot analysis of lysates prepared from HEK293T FcγR transfected with 3XFlag Rab5B or 3XFlag Rab5C and infected with *L.p.* WT or Δ*dotA* (MOI=20). *(Caption continued on next page.)*

(Figure 2.3 caption continued from previous page.) **(D)** Immunoblot analysis of Flag-Rab5A immunoprecipitation from *L.p.*-infected cells. HEK293T FcγR cells transfected with 3XFlag Rab5A and HA-ubiquitin (or vector control) were infected with WT or Δ*dotA* (MOI=20) for 4 hours or left uninfected. After Flag pulldown, input and IP samples were probed with anti-HA and anti-Flag antibodies. **(E)** Immunoblot analysis of ubiquitin immunoprecipitation from *L.p.*-infected cells. HEK293T FcγR cells transfected with 3XFlag Rab5A were infected with WT or Δ*dotA* (MOI = 20) for 4 hours or left uninfected. Ubiquitinated proteins were enriched from these samples using ubiquitin affinity beads (SignalSeeker Kit, Cytoskeleton Inc). Input and IP samples were probed with anti-Flag and anti-ubiquitin antibodies. Asterisk (*) indicates a non-specific band. (**F**) and **(G)** Immunofluorescence analysis of mCherry Rab5A WT or ΔCAAX LCV recruitment. HeLa FcγR cells were transfected with indicated construct, then infected for 1 hour with either WT or Δ*dotA L.p.* (MOI = 1), fixed, and stained with anti-*Legionella* antibody. **(F)** Representative images, and **(G)** quantification of biological replicates (N=3, adj. p-value = 0.008). 80-120 LCVs were scored per replicate as positive or negative for mCherry, and the percent mCherry+ LCVs was calculated per replicate. **(H)** Immunoblot analysis of ubiquitination of Rab5A WT vs ΔCAAX during *L.p.* infection. HEK293T FcγR cells were transfected with either 3X Flag Rab5A WT or ΔCAAX, then infected with WT or Δ*dotA L.p.* (MOI = 20) for 4 hours or left uninfected. Lysates were probed with anti-Flag and anti- Hsp70 antibody. **(I)** Quantification of normalized Rab5A ΔCAAX mUb intensity as a percent of Rab5A WT mUb during WT *L.p.* infection (see Methods). Biological replicates (N=4) were carried out as in (H).

we observe both a discrete band at ~37 kDa when blotting for HA, as well as higher molecular weight species, corresponding to mono- and poly-ubiquitinated Rab5A, respectively (**Fig 2.3D**). Pulldown on endogenous ubiquitin from cells expressing Flag-Rab5A also shows the accumulation of mono- and poly-ubiquitinated Rab5 in WT infected cells (**Fig 2.3E**).

Given the distinctive prolonged Rab5 association with the WT LCV in comparison to the Δ*dotA* LCV, we wanted to determine whether ubiquitination required Rab5 membrane localization. Two adjacent cysteine residues comprising a CAAX motif at the C-terminus of Rab GTPases are prenylated, and these lipid moieties insert into target membranes[69]. We generated mCherry tagged Rab5A WT and lipid anchor deletion (Rab5A ΔCAAX) constructs, and quantified localization to the WT and Δ*dotA* LCVs during infection in HeLa FcγR. Rab5A WT localizes to both the WT and Δ*dotA* LCV, whereas Rab5A ΔCAAX is diffuse and excluded from the LCV (**Fig 2.3F-G**). Flag-tagged versions of these constructs show a clear loss of ubiquitination (as read out

by monoubiquitination) for the ΔCAAX construct (**Fig 2.3H-I**), consistent with the model that Rab5A ubiquitination requires membrane association.

Effectors SidC/SdcA are Required for Rab5 LCV Localization and Ubiquitination

Next, we sought to identify bacterial effectors required for Rab5A ubiquitination. Previous studies have shown that bacterial effector paralogs SidC and SdcA are required for Rab1[47] and Rab10[48] ubiquitination. To determine if SidC/SdcA play similar roles in Rab5 ubiquitination, we infected HEK293T FcγR cells expressing Flag-Rab5A with SidC/SdcA knockout and complemented strains. Indeed, infection with a SidC/SdcA genomic deletion strain (*L.p. ΔsidC/sdcA*) fails to induce Rab5A ubiquitination, as indicated by the loss of mono-ubiquitinated species (**Fig 2.4A-B**). Transformation of the Δ*sidC/sdcA* strain with a plasmid encoding either SdcA or SidC is sufficient to rescue Rab5A monoubiquitination, suggesting that these effectors are functionally redundant in this context. SdcA/SidC have been identified as E3 ligases with unique protein folds[46]. While these proteins catalyze autoubiquitination *in vitro*, neither direct *in vitro* ubiquitination assays with SidC and Rab1 nor several mass spectrometry-based approaches have revealed host target proteins of SidC/SdcA[46,70]. In accordance with these findings, ectopic expression of SidC or SdcA in the absence of infection is not sufficient to induce Rab5A monoubiquitination (**Fig 2.4C**). This result suggests that the context of infection provides the complete enzymatic machinery required for SidC/SdcA-mediated Rab5 monoubiquitination, which could include either bacterial or host components, or both.

As SidC/SdcA are required for the recruitment of Rab1[47] and Rab10[48], we next examined whether SidC/SdcA control Rab5A recruitment. Immunofluorescence analysis reveals that the Δ*sidC/sdcA* LCV fails to accumulate endogenous Rab5A at 1hpi, whereas Δ*sidC/sdcA* strains complemented with either SidC- or SdcA- expressing plasmids robustly recruit Rab5A (**Fig 2.4D-E**). The finding that bacterial effectors recruit Rab5A is somewhat surprising, as Rab5 activity is generally thought to be deleterious to *L.p.* infection[59,71].

18
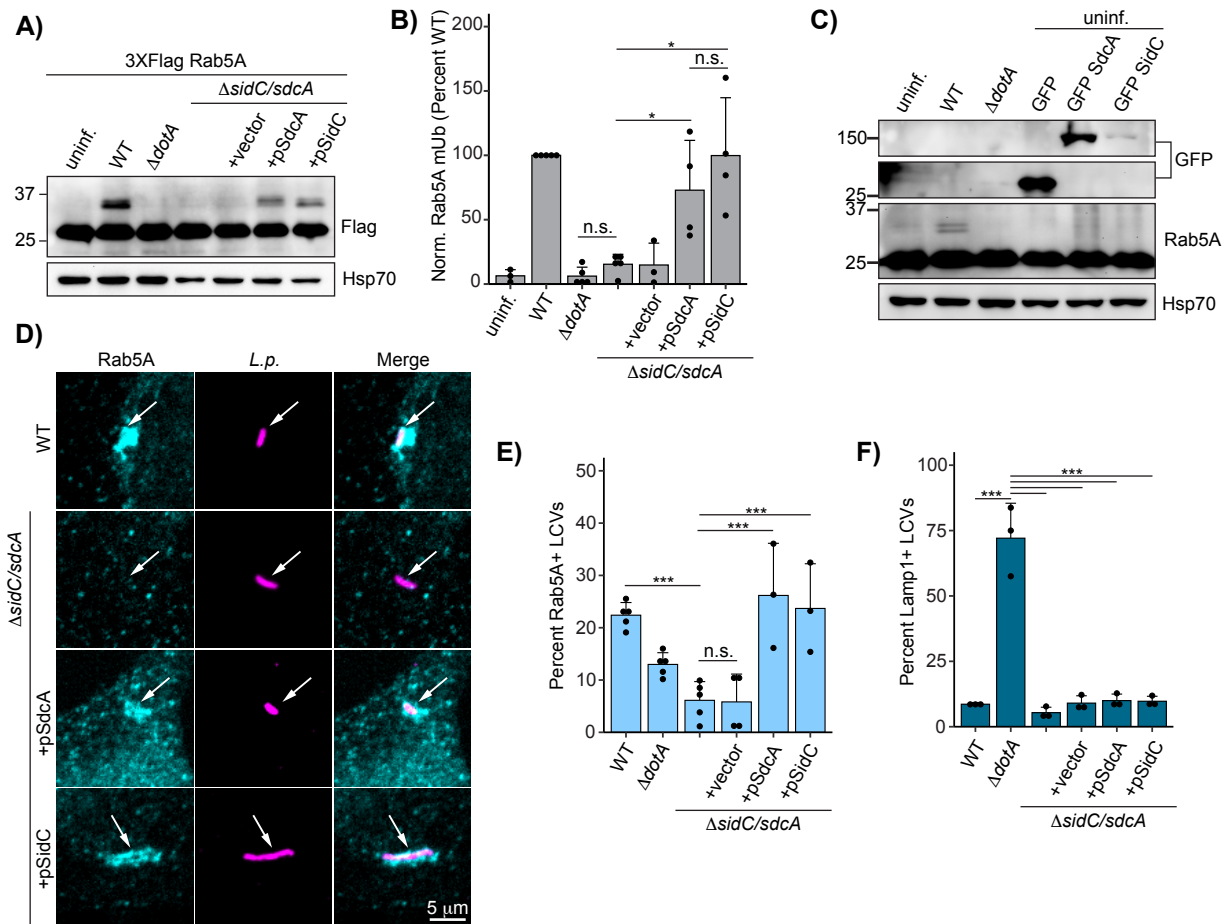
Figure 2.4 SidC/SdcA are required for Rab5 ubiquitination and LCV recruitment.

(A) Rab5A monoubiquitination during infection with *L.p.* Δ*sidC/sdcA* strain panel (WT, Δ*dotA*, Δ*sidC/sdcA*, and Δ*sidC/sdcA* transformed with vector or plasmid expressing SdcA or SidC). HEK293T FcγR expressing 3XFlag Rab5A were infected with the indicated strain or left uninfected. Cells were lysed at 4hpi and probed with anti-Flag antibody. **(B)** Quantification of biological replicates (N=3-5) of experiment shown in (A). Normalized Rab5A monoubiquitination intensity was calculated as a percentage of *L.p.* WT infection levels (see Methods), (N=3-4). **(C)** Immunoblot analysis of Rab5A during SdcA or SidC ectopic expression. HEK293T FcγR were either left untransfected (lanes 1-3) or transfected with GFP alone or GFP-tagged SdcA or SidC. The untransfected cells were either left uninfected or infected with *L.p.* WT or Δ*dotA* (MOI = 20) for 4 hours. All cells were lysed and probed with anti-Flag, anti-GFP, and anti-Hsp70 antibodies. **(D)** Representative images of Rab5A LCV recruitment levels for the Δ*sidC/sdcA* strain panel. HeLa FcγR cells were infected with indicated strain (MOI=1) for 1 hour, fixed, and probed with anti-*Legionella* and anti-Rab5A antibodies. **(E)** Percent Rab5A+ LCVs for experiments described in (D) (N=3-5, 75-150 LCVs per replicate, adj. p-value = 0.003) **(F)** Quantification of Lamp1 LCV recruitment for the Δ*sidC/sdcA* strain panel. HeLa FcγR cells were infected with indicated strain (MOI=1) for 4 hr, fixed, and probed with anti-*Legionella* and anti-Lamp1 antibodies. LCVs were scored as in (E).

The Δ*sidC/sdcA* strains are as resistant to lysosomal fusion as WT *L.p.* (**Fig 2.4F**), consistent with a model in which Rab5 recruitment and ubiquitination are not a primary mechanism of endosome maturation subversion at the LCV membrane.

The SidE Family Contributes to Rab5 Polyubiquitination and Membrane Retention

We next sought to identify additional effectors involved in Rab5 ubiquitination. Recent work has linked both the LCV recruitment and ubiquitination of Rab33b to the activity of non-canonical ligase effectors in the SidE family (SidE, SdeA, SdeB, SdeC)[72], leading us to hypothesize that the SidE family may play similar roles to SidC/SdcA in the recruitment and ubiquitination of small GTPases during infection. To test if SidE family effectors influence Rab5 ubiquitination, immunopurified Flag Rab5 as in section 2 (Fig 1.3D) from HEK293T FcγR cells infected with WT *L.p.*, Δ*dotA*, and SidE family knockout or complemented strains. Strikingly, SidE family knockout shows no effect on Rab5 monoubiquitination but diminished high molecular weight polyubiquitinated species (**Fig 2.5A-B**). Notably, SidC/SdcA knockout abrogates both mono- and polyubiquitination for Rab5 (**Fig 2.5A-B**), suggesting that SidE family-mediated polyubiquitination may lie downstream of SidC/SdcA activity.

We next assessed if the SidE family of effectors is necessary for Rab5 recruitment to the LCV. Immunofluorescence analysis shows that the Δ*sidE/sdeABC* LCV fails to accumulate endogenous Rab5A at 1hpi, whereas an Δ*sidE/sdeABC* strain complemented with SdeB expressing plasmid robustly recruits Rab5A (**Fig 2.5C-D**). This result suggests that Rab5 monoubiquitination, which is unaffected by the absence of SidE family effectors, is not sufficient to retain Rab5 in the LCV membrane.

With poly-ubiquitination but not mono-ubiquitination associated with the retention of Rab5 in the LCV membrane, we hypothesized that polyubiquitinated Rab5 may associate more stably with cellular membranes. To test this hypothesis, we performed subcellular fractionations of cells
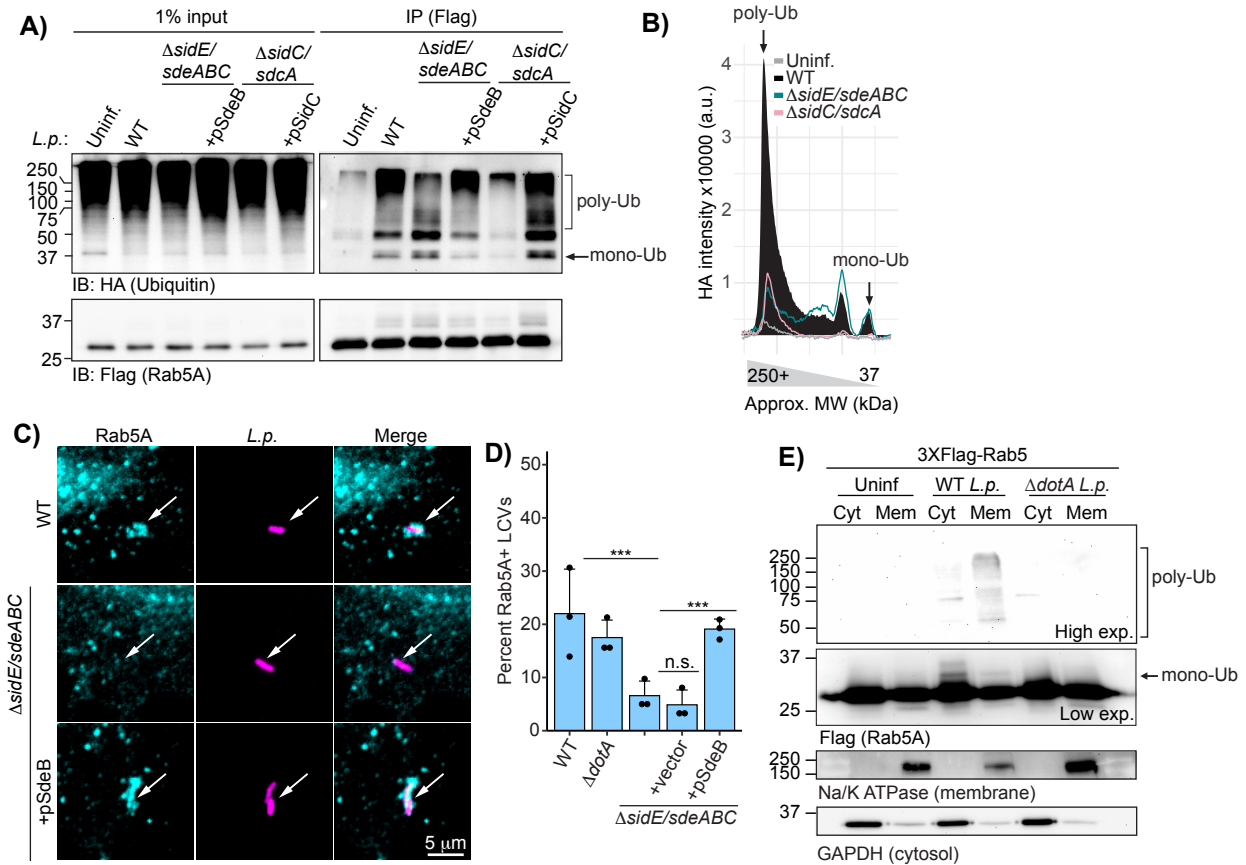
Figure 2.5 The SidE family is required for Rab5 polyubiquitination and membrane retention.

(A) Immunoblot analysis of Flag-Rab5A immunoprecipitation from cells infected with SidE family and SidC/SdcA strain panel. HEK293T FcγR cells transfected with 3XFlag Rab5A and HA-ubiquitin were infected with *L.p.* WT, Δ*sidE/sdeABC*, Δ*sidC/sdcA,* and appropriate plasmid complemented strains (MOI = 20) for 4 hours or left uninfected. After Flag pulldown, input and IP samples were probed with anti-HA and anti-Flag antibodies. **(B)** Plot profiles of HA signal shown in IP panel in (A) for uninfected and *L.p.* WT, Δ*sidE/sdeABC*, and Δ*sidC/sdcA* infected samples. **(C)** Representative images of Rab5A LCV recruitment levels for the Δ*sidE/sdeABC* strain panel as observed by immunofluorescence. HeLa FcγR cells were infected with indicated strain for 1 hour, fixed, and probed with anti-*Legionella* and anti-Rab5A antibodies. **(E)** Quantification of biological replicates (N=3, adj. p-value = 0.005) of experiment shown in (D). 60-120 LCVs were scored per replicate as positive or negative for Rab5A recruitment, and the percent Rab5A+ LCVs was calculated per replicate. **(E)** immunoblot analysis of cellular fractionations performed on HEK293T FcγR cells transiently expressing Flag-tagged Rab5 and infected with *L.p.* WT or Δ*dotA* (MOI =20) or left uninfected. Cells were infected for 1 (E) or 4 (F) hours.

expressing Flag-Rab5 and infected with *L.p.* WT or Δ*dotA*. Monoubiquitinated Rab5 is distributed between the membrane and the cytosol, whereas the higher molecular weight polyubiquitinated species are specifically enriched in the membrane fraction (**Fig 2.5E**). Taken together, our data suggests that polyubiquitination is required for stable Rab5 membrane localization during infection.

Discussion

In Chapter 2, we explore the relationship between *L.p.* and the host endolysosomal system by focusing on Rab5, the master regulator of the early endosomal compartment. Previously published results conflicted on whether Rab5 associates with the WT LCV[28,30]. In the present study we relied on immunofluorescence analysis of endogenous Rab5 during infection and found that the WT LCV stains positive for Rab5A at moderate frequencies throughout early infection. Additionally, we link Rab5 ubiquitination to LCV recruitment, and observe ubiquitination of endogenous Rab5 in U937 macrophage-like cells. Notably, previous reports suggest that overexpression of Rab5 antagonizes *L.p.* pathogenesis but does so by decreasing the integrity of the LCV membrane[59,71], rather than by increasing trafficking of the LCV to the lysosome. Consistent with this finding, we observe that Rab5A overexpression results in a bacterial replication defect without an increase in Lamp1 recruitment to the WT LCV. Taken together, these results are inconsistent with a model by which Rab5 activity simply increases trafficking of the LCV to the lysosome, and instead suggest a nuanced interplay between *L.p.* effectors and Rab5 activity during infection.

We discover that Rab5 is both poly and mono-ubiquitinated during *L.p.* infection, and that ubiquitin ligase bacterial effectors SidC and SdcA are required for both Rab5A LCV recruitment and ubiquitination. This result adds Rab5A to the list of GTPases already known to be LCV recruited by SidC/SdcA (Arf1, Rab10), and GTPases whose ubiquitination is known to be controlled by SidC/SdcA (Rab1, Rab10)[47,48]. We find that the SidE family of bacterial effectors
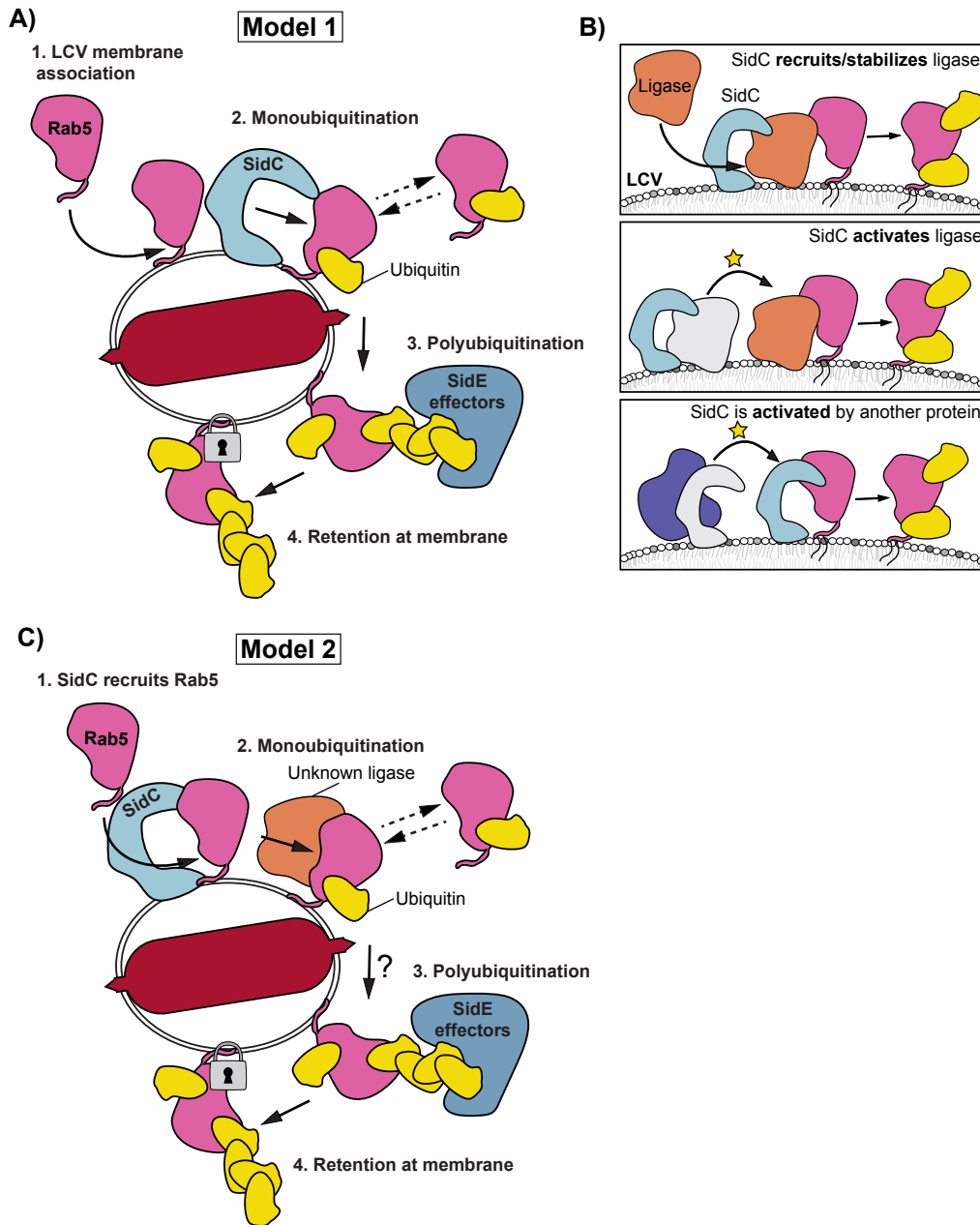
Figure 2.6 Models of Rab5 regulation by SidC/SdcA and SidE family effectors.

(A) Model 1: sequential activity of SidC/SdcA and SidE effector families could explain our experimental observations. **(B)** Several models of SidC/SdcA mediated Rab5A ubiquitination. **(C)** Model 2: SidC/SdcA could instead be responsible for Rab5 recruitment, potentially uncoupling Rab5 monoubiquitination and SidE family-mediated polyubiquitination.

contribute to high molecular weight polyubiquitination – but not monoubiquitination – of Rab5, and that polyubiquitinated Rab5 is membrane associated. Combined with the observation that the SidE family is required for Rab5 recruitment to the LCV, this data leads us to hypothesize that ubiquitination is at least in part a means to retain Rab5 in the bacterial vacuole membrane. Recent work on a *L.p.* effector DUB, Lem27/LotC, is consistent with this model, showing that overexpression of Lem27/LotC reduces both poly- and monoubiquitination of Rab10 during infection, and also suppresses Rab10 association with the LCV[48]. Notably, knockout of SidE/SdeA/B/C does not completely prevent polyubiquitination of Rab5 (**Fig 2.5A**), indicating that other effectors play a role in polyubiquitination. However, the Δ*sidE/sdeABC* strain LCV is largely Rab5-negative, suggesting that non-canonical PR-ubiquitination may play a specific role in maintaining Rab5 at the LCV membrane.

Several models can explain the observations made in this study on the relationship between Rab5 membrane association, mono- and polyubiquitination, and the SidE and SidC family of effectors. One possibility is that Rab5 is initially recruited to the LCV membrane, monoubiquitinated in a SidC dependent manner, at which point Rab5 is not stably membrane associated, and then is further ubiquitinated by the SidE family of effectors, which results in stable membrane association (**Fig 2.6A**). In this scenario, it remains to be determined whether Rab5 is recruited to the LCV membrane by host or bacterial factors. Rab5 LCV membrane association could also be part of a host attack on *L.p.*, and subsequent effector driven ubiquitination part of a containment strategy to limit Rab5 activity. This hypothesis would be in line with the small but significant growth defect observed during Rab5 overexpression, and improved bacterial replication observed upon Rab5 knockdown by others[71]. Another question raised by this first model is how SidC/SdcA might induce Rab5 monoubiquitination (**Fig 2.6B**). Multiple studies have shown that these effectors are capable of both autoubiquitination[46] and ubiquitin utilization[73,74] *in vitro* in the presence of E1 and E2 enzymes. The catalytic residues required for SidC autoubiquitination are also necessary for SidC dependent phenotypes during infection, such as

the recruitment of ER membrane to the LCV[46]. However, several lines of evidence suggest that small GTPases may not be a direct target of SidC/SdcA ubiquitin ligase activity. First, ectopic expression of SidC/SdcA does not induce ubiquitination of Rab1[46,47] or Rab5 (this study), despite being necessary for Rab1/5 ubiquitination during infection. Second, *in vitro* ubiquitination reactions containing purified SidC have not resulted in Rab1A ubiquitination[46]. Lastly, protein-protein interaction experiments did not find interaction between SidC/SdcA and Rab1, Arf1, or numerous other proteins involved in LCV formation[47], and several mass spectrometry-based approaches have failed revealed host target proteins of SidC/SdcA ligase activity during ectopic expression[46,70]. Perhaps SidC requires the context of infection to ubiquitinate Rab5, such as the presence of other bacterial effectors or host proteins. Alternatively, SidC may ubiquitinate another host or bacterial protein, or simply itself, during infection, which indirectly leads to the recruitment or stabilization of an enzyme to the LCV that then monoubiquitinates Rab5.

A second model consistent with the data presented here posits that SidC is required for the initial recruitment of Rab5 to the LCV membrane, and then both mono- and polyubiquitination are downstream of SidC activity, with SidC not directly ubiquitinating Rab5 at all (**Fig 2.6C**). In this case, mono- and polyubiquitination might be sequential steps, as proposed in model 1, or entirely independent. This model presupposes another ubiquitinating enzyme, either host or bacterial, that monoubiquitinates Rab5, as the SidE family knockout strain has no defect in Rab5 monoubiquitination (Fig 2.5). To date, eleven *L.p.* effector proteins with canonical E3 ligase activity aside from the SidC family have been discovered, so this is not a far-fetched hypothesis[43].

Several essential questions remain unanswered by either model. How polyubiquitination results in membrane retention of Rab5 is as yet unknown. Rab5 ubiquitination has been observed outside of the context of infection during ubiquitin overexpression, which results in monoubiquitination at multiple lysine residues. The authors determined that monoubiquitination at K140 and K165 depressed localization of Rab5 to endosome membranes, and interfered *in vitro* with binding to interaction partners and GDP release, respectively[75]. While the authors focus

on monoubiquitination, many Western blots included show high molecular weight Rab5 species that likely correspond to polyubiquitination (see Fig. 1E, for example). This work demonstrates that host ubiquitin ligases can ubiquitinate Rab5 outside of the context of infection, but with apparently different outcomes in terms of membrane localization. It is possible that this difference stems largely from the unusual nature of the PR-ubiquitination catalyzed by the SidE family of effectors. However, we have not directly demonstrated that Rab5 is in fact PR-ubiquitinated by the SidE family; it is possible that the SidE family of effectors indirectly induce Rab5 polyubiquitination and membrane retention. In fact, an initial paper describing SidE family activity found that Rab5 was not modified by SdeA[50], although in this case the authors relied on ectopic expression of SdeA, and there is evidence that SidE family members have some differences in specificity[18].

Altogether, this work reveals a complex interplay between two families of *L.p.* effectors that regulate hallmarks of the intracellular *L.p.* life cycle. The surprising finding that bacterial effectors recruit Rab5 to the LCV opens a host of mechanistic questions; in particular, how does this benefit *L.p.*? Our data suggests that Rab5 is not functioning as it usually would at an early endosome membrane given the exclusion of EEA1, and this is consistent with previous findings that the LCV is resistant to fusion with early endosomes in the time window of Rab5 recruitment found in our study[34]. We can speculate that Rab5 recruitment and ubiquitination may serve to contain and inactivate Rab5 at the LCV membrane. Recruitment could also stimulate the activity of effectors such as VipD, which is activated by binding Rab5-GTP[31]. Alternatively, Rab5 recruitment could be incidental - the coating of the LCV in ubiquitinated proteins during early infection is not well understood, and it is possible that any proteins that come into close contact with the LCV membrane, whether actively recruited or by chance, are ubiquitinated. It is perhaps telling that SidC/SdcA are required for the recruitment of both ubiquitin[47] and Rab5 to the LCV. In Chapter 3, we further explore the hypothesis that Rab5A is incorporated into a protective structure around the LCV during early infection.

CHAPTER 3 : LEVERAGING RAB5 AS A TOOL TO STUDY HOST PROTEINS AT THE LCV MEMBRANE

Introduction

In addition to acute targeting of eukaryotic host regulatory molecules, it has been proposed that intravacuolar pathogens secrete effectors that broadly maintain the integrity of their vacuole membranes throughout infection. These effectors, known as vacuole guards, play an essential role in protecting the vacuole during early infection[55]. Recently, the SidE family of effectors have been proposed to act as vacuole guards, both by generating a PR-ubiquitinated reticulon4 barrier around the LCV[59], and by phosphoribosylating polyubiquitin chains around the LCV to mask them from ubiquitin binding autophagy adaptors such as p62[60]. These findings are of particular interest, given the SidE family's role in locking Rab5 at the LCV membrane as discussed in Chapter 2, as it could suggest that Rab5 is being incorporated into a PR-ubiquitinated wall around the LCV. We realized that we had inadvertently discovered a useful tool for studying how proteins localized to the LCV membrane behave, as, to our knowledge, Rab5 is the only host protein that can be found on both the WT and ∆*dotA* LCV in the same time window during infection. We find that Rab5 has a distinctive, "cloud"-like morphology around the WT LCV, whereas the Rab5 localized to the ∆*dotA* LCV conforms closely to the bacterial cell body. The generation of this cloud is not predominately dependent on Rab5 regulatory proteins, but rather on the activity of the SidE family of effectors. We determine that Rab5 is exceptionally stable when localized to the WT LCV, resisting harsh detergent washout, whereas endosome and ∆*dotA* LCV-associated Rab5 is efficiently cleared by this treatment. These findings suggest that Rab5 is a component of an unusually stable structure around the WT LCV, and lay the groundwork for further study of the unique composition and properties of the shield around *L.p.*

WT LCV-associated Rab5 has a Distinctive "Cloud" Morphology

While analyzing Rab5 immunofluorescence images of infected cells, we observed that Rab5 localization patterns to the WT versus Δ*dotA* LCV were discernibly different by eye. While the Rab5 positive region around the Δ*dotA* LCV tends to overlay tightly with the bacterial cell, the Rab5 positive region associated with the WT LCV extends outward into a cloud-like area around the LCV (**Fig 3.1A**). To quantify this, we used CellProfiler image analysis tools to measure the
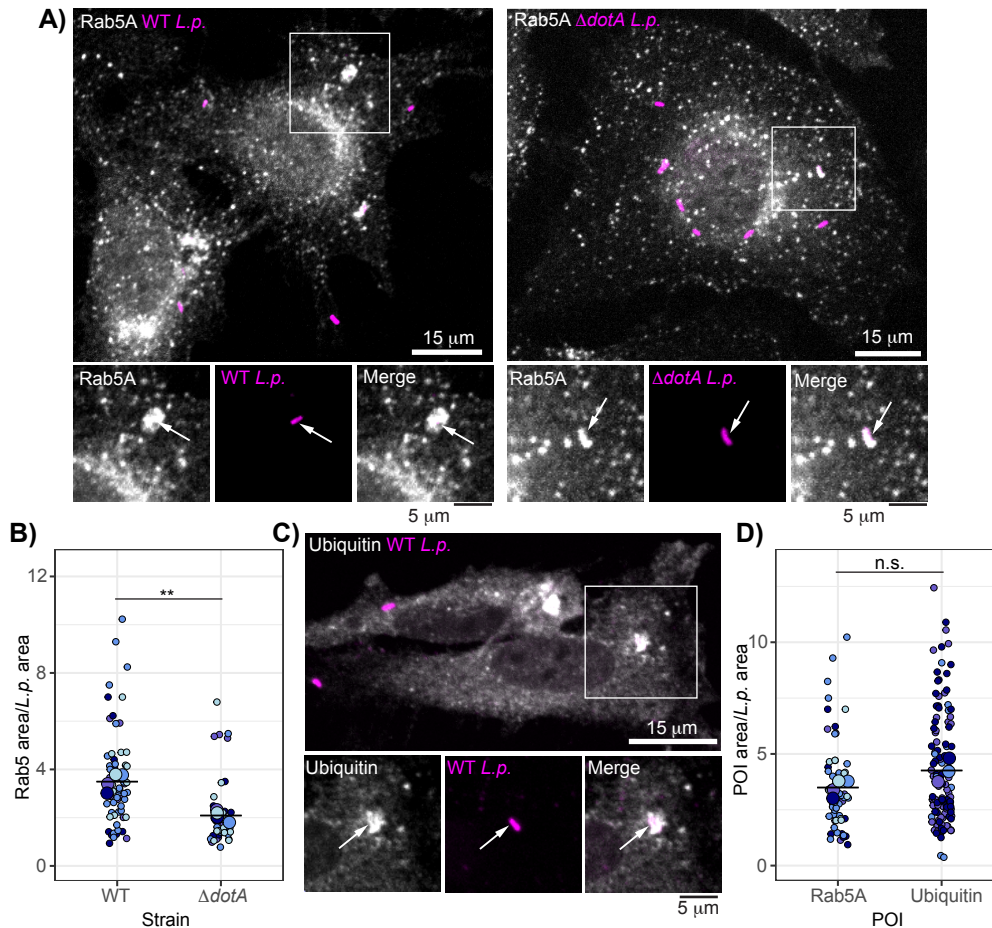
Figure 3.1 WT LCV-associated Rab5 exhibits a "cloud" morphology.

(A) Representative immunofluorescence images of Rab5 morphology at the WT and Δ*dotA* LCV at 1 hpi (MOI=1). **(B)** Quantification of normalized Rab5 area at the WT and Δ*dotA* LCV at 1hpi. Welch's t-test for mean of biological replicates (N=4 10-20 LCVs/rep for each strain), ** = p<0.005 **(C)** Representative immunofluorescence image of ubiquitin conjugate (FK2) recruitment to the WT LCV at 1hpi (MOI=1). **(D)** Quantification of normalized Rab5 and ubiquitin area at the WT LCV at 1hpi. Statistical analysis as in (B), n.s. = p>0.05.

area ratio of the Rab5+ region around the LCV to the bacterial cell. We find across biological replicates that the WT LCV-associated Rab5+ region is larger than that surrounding the $\Delta dotA$ LCV (**Fig 3.1B**). This expansive localization around the LCV is not unique to Rab5, although to our knowledge it has never been quantified. "Cloud"-like localization of host proteins is visible in micrographs of Rab6A and Rab33B[72], reticulon4[18], and ubiquitin[54] in previous publications. We have reproduced the ubiquitin "cloud" localization (**Fig 3.1C**), and, applying the same morphology analysis described above for Rab5, find that the ubiquitin and Rab5 "clouds" extend out from the LCV to similar degrees (**Fig 3.1D**).

The SidE family of Effectors Control "Cloud" Size

As discussed in the introduction to Chapter 1, Rab5 activation is controlled by its GEF, Rabex5. Additionally, Rab5 activation is propagated by one of its binding partners, Rabaptin5, which binds Rab5-GTP and recruits more Rabex5 to the endosomal membrane[76]. To determine whether hyperactivation of either of these host regulators contribute to Rab5 recruitment and cloud formation at the LCV membrane, we overexpressed GFP-tagged constructs of each and infected cells with either *L.p.* WT or $\Delta dotA$ for one hour. To ensure that our constructs were in fact stimulating Rab5 activity, we measured endosome size in uninfected cells, as endosome enlargement is a hallmark of high Rab5 activity[77–79]. We find that overexpression of both Rabaptin5 and Rabex5 constructs significantly increase endosome size in comparison to EGFP only transfected cells (**Fig 3.2A-B**). Intriguingly, overexpression of Rabex5, but not Rabaptin5, increases the fraction of $\Delta dotA$ LCVs that score positive for Rab5. However, the frequency of WT LCV Rab5 positivity is not affected by either construct (**Fig 3.2C**). This is not due to exclusion of Rabex5 from the WT LCV, as the WT LCV scores positive for Rabex5 at higher frequencies than the $\Delta dotA$ LCV (**Fig 3.2D**). Finally, neither Rabex5 nor Rabaptin5 overexpression increases the area of the Rab5+ cloud around the WT LCV, indicating that these proteins are not the predominate drivers of cloud formation (**Fig 3.2E**).
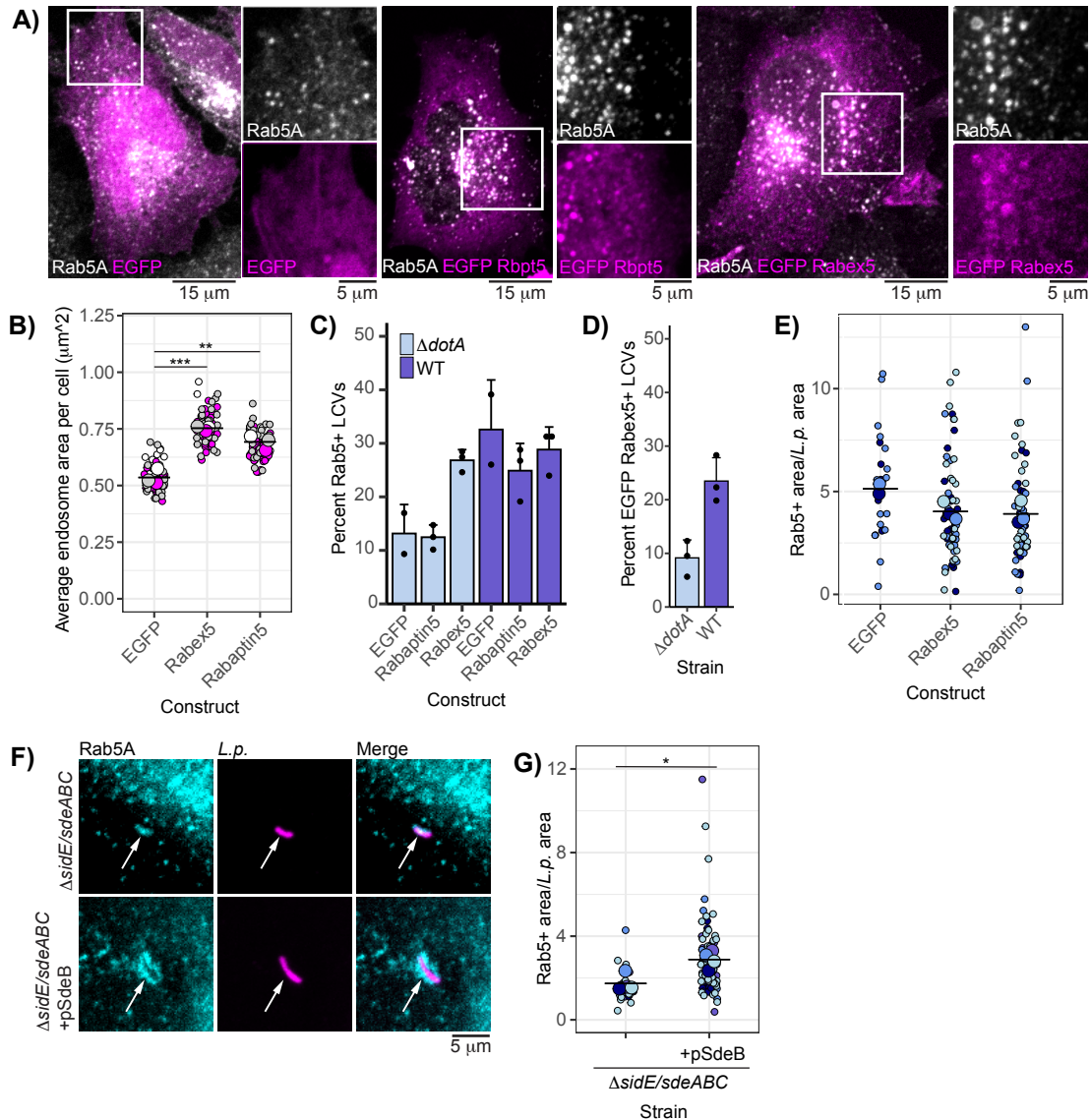
Figure 3.2 The SidE family of effectors, not host regulators, control Rab5 cloud formation.

(A) Representative images of Rab5A in uninfected HeLa FcγR cells expressing the indicated EGFP-fusion construct or EGFP alone. **(B)** Mean endosome area per cell in HeLa FcγR cells expressing the indicated EGFP-fusion construct or EGFP alone. N= 3, 20-25 cells per replicate. Means for replicates were subjected to ANOVA followed by Tukey-Kramer post-hoc test, ** = $p<0.005$, *** = $p<0.0005$. **(C)** Percent Rab5A+ LCVs at 1hpi with *L.p.* WT or Δ*dotA* (MOI=1) in HeLa FcγR cells expressing the indicated construct. **(D)** Percent EGFP Rabex5+ LCVs at 1hpi. **(E)** WT LCV-associated Rab5A area normalized to *L.p.* area in HeLa FcγR cells expressing the indicated EGFP-fusion construct or EGFP alone. N = 2-3, 10-20 LCVs per replicate. **(F)** Rab5 association with SidE family KO strain vs. SdeB complemented (MOI =1). **(G)** LCV-associated Rab5A area normalized to *L.p.* area for experiment described in (F), N= 4, 10-20 LCVs scored per replicate. Replicate means were subjected to Welch's t-test, * = $p<0.05$.

30

As host regulatory factors do not appear to be a primary driving force in Rab5 cloud formation around the LCV, we next examined the role of bacterial effectors in Rab5+ LCV morphology. In Chapter 2, we demonstrated that the SidE family of non-canonical ubiquitin ligase effectors are required for both polyubiquitination and efficient recruitment of Rab5 to the LCV (**Fig 2.5**). While the SidE family knockout strain has a strong Rab5 recruitment defect, about 5-10% of the mutant LCVs are Rab5 positive. In examining these few positive mutant LCVs, we find that the Rab5 localization to the Δ*sidE/sdeABC* LCV resembles that of the Δ*dotA* LCV, with Rab5 signal largely confined to the bacterial cell area. Complementation of the knockout strain with plasmid-encoded SdeB rescues the Rab5 cloud phenotype (**Fig 3.2F-G**).

WT LCV-associated Rab5 is Detergent Resistant

As we have determined that Rab5 associated with the WT LCV has distinctive morphological properties, and that polyubiquitinated Rab5 is stably membrane-associated (Fig 2.5), we next wanted to assess if WT LCV-associated Rab5 exhibited the same stability as "normal" membrane-associated Rab5. To this end, we determined whether Rab5 could be washed out with harsh detergent after fixation when localized to the WT LCV. It has been demonstrated that protein antigens localized to intracellular membranes can be disrupted by detergent permeabilization, whereas the gentler surfactant saponin, which disrupts the cholesterol-rich plasma membrane, largely preserves membrane-bound epitopes[80]. Previous work shows that the smooth ER protein reticulon4 is resistant to both ionic and nonionic detergents when associated with the WT LCV[18], but, as reticulon4 is not recruited to the Δ*dotA* LCV, there was no direct negative control for this experiment. We infected cells with *L.p.* WT or Δ*dotA*, fixed, and then permeabilized with either 0.5% saponin, as usual, or 5% sodium dodecyl sulfate (SDS), and carried out immunofluorescence analysis of endogenous Rab5A. To ensure our permeabilization strategy worked as expected, we measured the corrected total cell fluorescence (CTCF) of uninfected cells in both permeabilization conditions, and found that
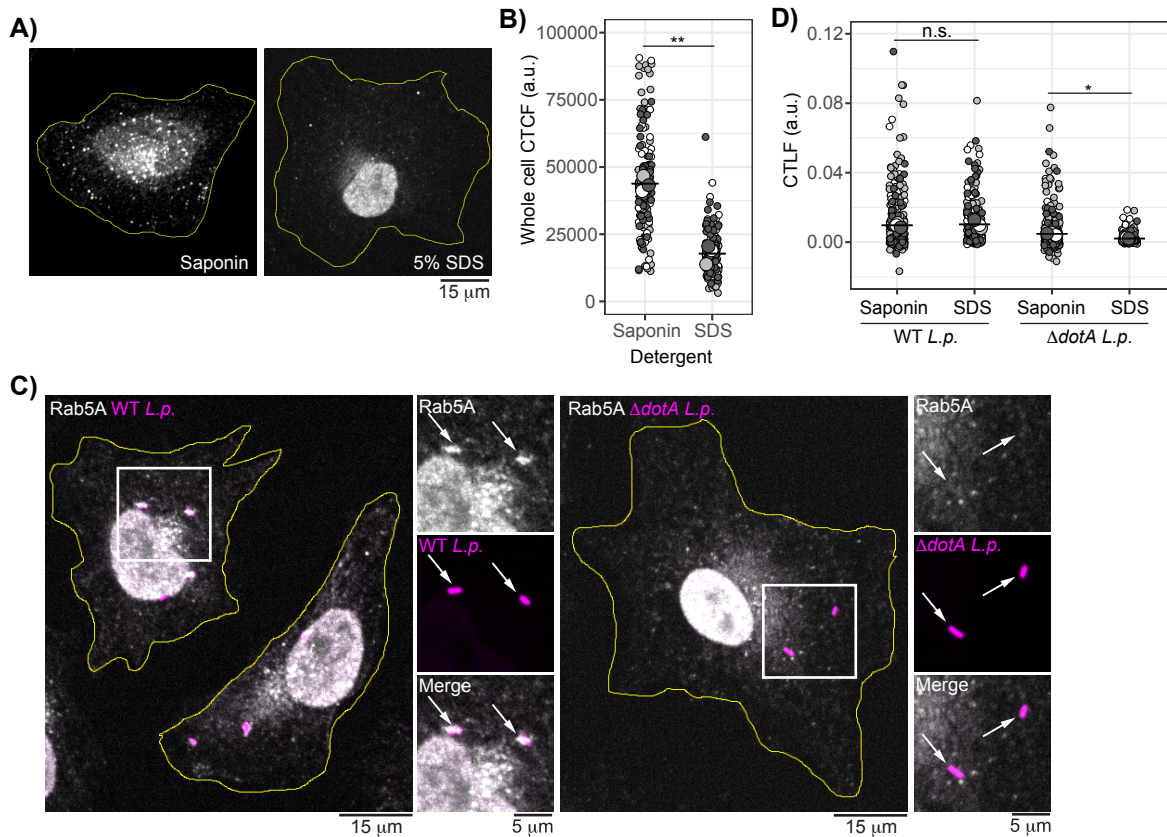
Figure 3.3 WT LCV-associated Rab5A resists detergent washout.

(A) Representative images of Rab5A in uninfected cells exposed to saponin vs. 5% SDS permeabilization. **(B)** Rab5A corrected total cell fluorescence (CTCF) for uninfected cells permeabilized as in (A). N = 3, 25 cells per replicate. Replicate means were subjected to Welch's t-test, **=$p<0.005$. **(C)** Representative images of WT and Δ*dotA* LCV Rab5A association at 1hpi (MOI=1) after 5% SDS permeabilization. **(D)** Rab5A corrected total LCV fluorescence (CTLF) for *L.p.* WT, Δ*dotA* for saponin and 5% SDS permeabilization. N=3, 20-30 LCVs scored/replicate. Replicate means were subjected to ANOVA with post-hoc Tukey-Kramer test. * = $p<0.05$, n.s. = $p>0.05$.

indeed, 5% SDS significantly reduced total Rab5A fluorescence (**Fig 3.3A-B**). On the other hand,

Rab5A associated with WT LCVs resisted 5% SDS washout, whereas no remaining Rab5A was

visible on Δ*dotA* LCVs (**Fig 3.3C**). To quantify this, we adjusted the CTCF calculation, measuring

the integrated Rab5A intensity within the LCV region and subtracting mean local background

multiplied by LCV area. We term this measurement corrected total LCV fluorescence, or CTLF.

Using this metric, we find that saponin and 5% SDS permeabilization produce equivalent Rab5A

CTLF values for *L.p.* WT, whereas 5% SDS significantly reduces the Δ*dotA* CTLF compared to saponin permeabilization (**Fig 3.3D**).

Discussion

In Chapter 3, we explore the special properties of Rab5 when associated with the WT LCV. We find that the morphology of WT LCV-associated Rab5 is distinct from Δ*dotA* LCV-associated Rab5, and in fact reminiscent of ubiquitin staining of the WT LCV. This cloud-like morphology is dependent on the activity of SidE family effectors, rather than Rab5 the activating proteins Rabex5 or Rabaptin5. Finally, we demonstrate that Rab5 is unusually stable when associated with the WT LCV, resisting washout with 5% SDS after fixation. In Chapter 2, we illustrated that Rab5 is stably membrane-associated when polyubiquitinated during infection, and this polyubiquitination was dependent largely on the SidE family of effectors. Importantly, the SidE family of effectors is also necessary for efficient recruitment of Rab5 to the LCV. Taken together, these results are consistent with a model in which SidE-mediated polyubiquitination of Rab5 incorporates Rab5 into a stable structure around the LCV, which is unlike Rab5 localization to a "normal" endosome (as represented by the Δ*dotA* LCV).

The chemistry of PR-ubiquitination may explain these experimental observations. The SidE family, unlike canonical ubiquitin ligases, forms a covalent link between an arginine side chain on ubiquitin and a serine residue on the target protein[49]. Canonical E3 ligases, on the other hand, conjugate the C-terminus of ubiquitin to the target protein, most frequently onto a lysine side chain[38]. The unique chemistry of the SidE family suggests the possibility that canonically ubiquitinated proteins could be crosslinked to other proteins by forming a bridge between an arginine on the ubiquitin molecule and serine on another protein. This hypothesis is attractive, as our mass spectrometry analysis establishes that Rab5 is canonically ubiquitinated during infection, and crosslinking could explain both the morphology and stability of Rab5 at the WT LCV membrane. This crosslinking model could also explain the finding that both SidC/SdcA and the

SidE family of effectors are required for Rab5 retention at the LCV. If SidC/SdcA is required for canonical ubiquitination of Rab5A, either directly or indirectly as discussed in Chapter 2, these effectors would work upstream of the SidE family crosslinking activity, and as such as be a requirement for stable cloud formation. Further investigation into this hypothesis is warranted, as it will reveal heretofore elusive cell biological functions of the SidE family of effectors at the LCV during infection.

CHAPTER 4 : AN ALTERNATIVE MODEL FOR SIDC/SDCA MODE OF ACTION

Introduction

Modulation of ubiquitin signaling is a central element of *L.p.* infection. Multiple *L.p.* effectors with canonical and noncanonical ubiquitin ligase activity have been identified, as well as a catalog of DUBs[43]. Intriguingly, it is well established that ubiquitinated substrates accumulate at the LCV throughout early infection in an effector-dependent manner[47,54,81]. For many intracellular bacterial pathogens, tagging with ubiquitin is a death knell, as it allows the host to recognize and enclose the bacterium in autophagic membranes and subsequently traffic the autophagosome to the lysosome[42]. *L.p.,* on the other hand*,* appears to have incorporated ubiquitin into core elements of its pathogenesis, such as efficient effector translocation through the T4SS[52] and vacuolar expansion during the late stages of infection[53]. Inhibition of the proteasome with MG132 inhibits intracellular growth[81]. Despite these advances, it is still unclear which proteins are incorporated into the ubiquitin coat around the LCV, whether these proteins are ubiquitinated at the membrane or elsewhere, whether ubiquitination is largely catalyzed by host or bacterial proteins, and what role the ubiquitin coat plays during infection. Analysis of our ubiquitinomics dataset (described in Chapter 2) reveals that *L.p.* infection induces an upregulation of ubiquitination specifically during early infection. This burst includes both host and bacterial substrates. Intriguingly, we find that SidC/SdcA are required for this massive upregulation in ubiquitination. Finally, we propose an alternative mechanism of action for SidC/SdcA; in addition to acting as unusual E3 ligases[46], they may regulate the activity of other *L.p.* effectors.

***Legionella* Infection Induces a Burst of Ubiquitination Events in Early Infection**

While the analysis of the ubiquitinomics mass spectrometry dataset focused on endosomal Rabs in Chapter 2, we detect hundreds of proteins with changes in ubiquitination compared to uninfected control in the WT *L.p.* infected samples. Filtering our data for hits with

|Log2(FC)|>1 compared to uninfected control and a p-value<0.05, we find that the largest effect of *L.p.* infection in terms of sheer number of modified host proteins occurs at 1hpi, with 420 total proteins ubiquitinated and 195 deubiquitinated (**Fig 4.1A**). By 8hpi, these numbers drop to 271 ubiquitinated and 189 deubiquitinated proteins. In comparison, changes in ubiquitination during Δ*dotA* infection are minimal at both timepoints. The burst of ubiquitination during early WT infection was of particular interest to us. Of the 420 total ubiquitinated proteins, 270 were imputed, meaning that the ubiquitination was not detected in the uninfected condition. While some imputed values are likely artifacts, many do have biological significance as observed for Rab5A in Chapter 2, suggesting that *L.p.* infection induces novel or uncommon ubiquitination events.

In addition to changes in the host ubiquitinome, our mass spectrometry analysis detected ubiquitination in the secreted *L.p.* proteome. We tabulated *Legionella* proteins that experience Log2(FC)>1 with a p-value<0.05 for both *L.p.* WT and Δ*dotA* in comparison to control at both 1- and 8-hpi. The few *L.p.* proteins showing deubiquitination were considered artifacts, as no *L.p.* protein should be ubiquitinated in the uninfected control condition. Very few *L.p.* proteins were detected in the Δ*dotA* condition, consistent with low levels of release of *L.p.* protein into the sample due to lysis of the bacterial cells. On the other hand, in the *L.p.* WT infected sample 36 effectors were detected as ubiquitinated at 1hpi, and 46 at 8hpi (**Fig 4.1B**). Only 6 and 4 non-effector proteins were detected at 1- and 8hpi, respectively, suggesting again that the majority of the detected *L.p.* ubiquitinome was secreted into the host cell. Examining only effector proteins ubiquitinated in the WT-infected conditions, we observe that the majority of effector proteins are detected at both timepoints, with 8 specific to 1hpi and 18 specific to 8hpi. Encouragingly, SidH, an effector known to be ubiquitinated by another effector, LubX, from 1hpi onwards[82], is detected as ubiquitinated at both 1- and 8hpi. Our data shows some correlation between the timepoint bacterial effectors have been shown to act and the timepoint at which we detect effector ubiquitination. For example, the effectors VpdC[53] and SdhA[59] function later in infection timepoints,
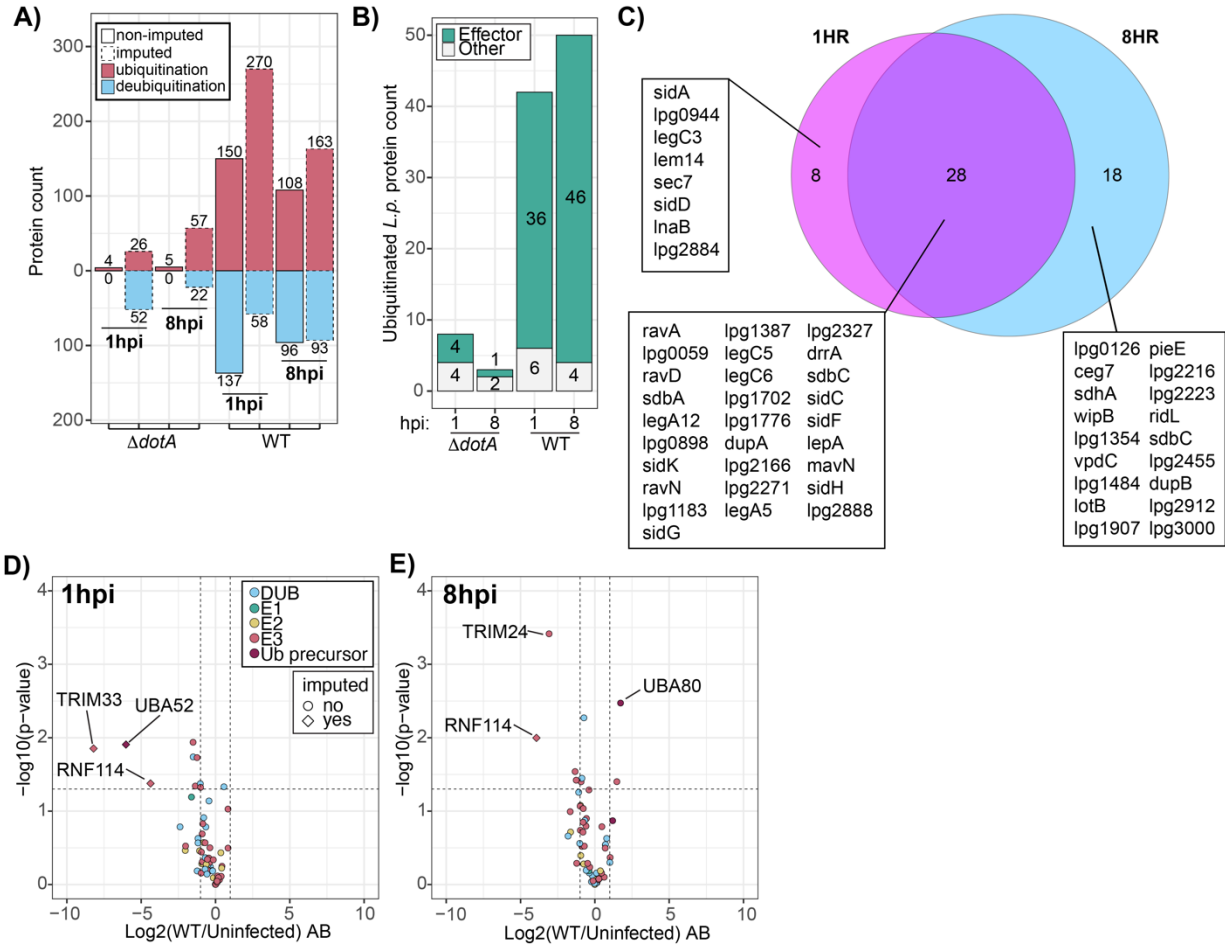
Figure 4.1 *L.p.* infection induces a burst of ubiquitination.

(A) Counts of host proteins meeting significance cutoff (p<0.05) with |Log2(FC)|>1 in the WT vs. uninfected and Δ*dotA* vs. uninfected conditions. **(B)** Counts of *L.p.* proteins with Log2(FC)>1 as in (A). **(C)** Comparison of *L.p.* effectors ubiquitinated during WT infection at 1 and 8hpi. **(D)** and **(E)** Volcano plot representation of abundance of ubiquitin-related host proteins during WT infection at 1- and 8hpi.

and their ubiquitination is only detected in the 8hpi samples. Ubiquitination of effector proteins has previously been implicated in efficient T4SS translocation[52], and more recently the effector VpdC was shown to be a phospholipase activated by binding to ubiquitin which promotes expansion of the LCV late in infection[53]. In addition to the enormous number of effector proteins that act directly on ubiquitin, these observations highlight the central role and often unexpected

role that ubiquitin plays in the *L.p.* infection cycle. Our data suggest that in addition to host proteins, *L.p.* effectors are also substrates in the early burst of ubiquitination during infection.

The early burst of ubiquitination activity could be a result of direct ligase activity from secreted bacterial effectors, or changes in the host ubiquitin conjugation machinery. To roughly examine this question, we mined the abundance dataset for changes in host proteins involved in ubiquitination. Proteins participating in the ubiquitination cascade include the two known ubiquitin activating E1 enzymes UBA1 and UBA6[83], 37 E2 enzymes (HGNC), and 377 E3 enzymes with confirmed activity towards ubiquitin[84]. Ubiquitin itself is encoded by four genes, which produce either head-to-tail polymeric ubiquitin repeats (UbB and UbC), or an N-terminal fusion of a single ubiquitin molecular to a ribosomal protein (UBA52 and UBA80)[83]. These four proteins were included as "Ubiquitin precursors". Finally, downregulation of DUBs could also produce an increase in ubiquitination, and so we included 99 annotated DUBs (HGNC). Filtering the ubiquitinomics dataset using these lists, we find that no ubiquitin system related proteins are significantly increased in abundance at 1hpi (**Fig 4.1D**). Several proteins decrease in abundance relative to control, but for most significant values this change is barely past the |Log2FC|>1 threshold. The three exceptions include two E3 ligases (TRIM33 and RNF114), and a ubiquitin precursor (UBA52). However, all three values are imputed, meaning that the peptides were not detected in the uninfected control. As the imputation strategy used assigns a random small number to the denominator of the Log2FC calculation, the magnitude of the Log2FC for imputed values is not biologically meaningful. In any case, degradation of E3 ligases and a ubiquitin precursor would not directly explain the observed ubiquitination burst. Similarly, most ubiquitin system proteins do not experience significant abundance changes at 8hpi (**Fig 4.1E**). Two exceptions are TRIM24, an E3 ligase, and UBA80, a ubiquitin precursor. TRIM24 is a negative regulator of p53, which responds to an array of cellular stresses[85], and TRIM24 can be degraded to allow accumulation of p53[86]. Thus, the downregulation of TRIM24 at late stages of WT *L.p.* infection may be part of a stress response to prolonged infection, rather than a targeted

manipulation of ubiquitin signaling by the bacterium. The slight upregulation of UBA80 is potentially interesting, although given the recent findings that *L.p.* infection induces a ribotoxic stress response[12], caution must be applied in interpreting changes in ribosomal protein abundance. Overall, this analysis indicates that the observed burst of ubiquitination during early WT infection cannot be explained by large changes in abundance of host ubiquitin system proteins. However, it does not rule out the possibility in activity changes in host DUBs or ligases during infection.

SidC/SdcA are Required for the Ubiquitination Burst

We were intrigued by the timing of the observed ubiquitination burst, as ubiquitinated proteins accumulate around the LCV starting early in infection[54,81]. It has been established that SidC and SdcA are required for this ubiquitin accumulation for at least the first few hours of infection[47]. To orthogonally confirm our mass spectrometry analysis and determine whether SidC/SdcA are required for the ubiquitination burst, we infected 293T FcγR for 1 or 8 hours with *L.p.* WT, Δ*dotA*, or Δ*sidC/sdcA*, or left the cells uninfected as a negative control. Increased high molecular weight ubiquitin conjugates are observed specifically in the samples infected with *L.p.*
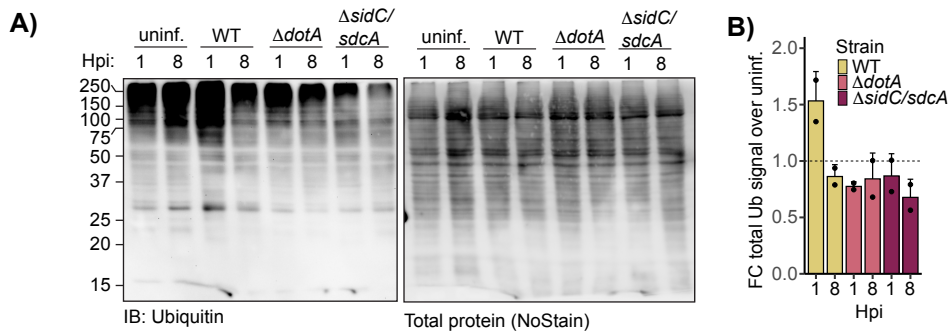
Figure 4.2 SidC/SdcA are required for the ubiquitination burst.

(A) Immunoblot analysis of the total pool of ubiquitinated proteins in 293T FcγR cells infected with *L.p.* WT, Δ*dotA*, or Δ*sidC/sdcA* (MOI = 20) for 1 or 8 hours, or left uninfected. Invitrogen NoStain protein labeling reagent was used to quantify total protein before immunoblot analysis. **(B)** Quantification of blots as in (A). Total ubiquitin signal was first normalized to total protein for each sample, then the fold change over the appropriate uninfected sample was calculated (N=2).

WT for 1 hour (**Fig 3.2A**). To quantify this phenomenon, total lane integrated density was normalized to total protein for each condition, and then the fold change over the corresponding uninfected sample was calculated (**Fig 3.2B**). While this assay is less sensitive than the mass spectrometry analysis and fails to capture more subtle variations between samples, these results confirm the burst in ubiquitination during early *L.p.* WT infection and illustrate that SidC/SdcA are indeed required for the initial upregulation of ubiquitination upon infection.

SidC/SdcA as Metaeffectors

The finding that SidC/SdcA are essential for the burst of ubiquitination during early infection is interesting, given that no direct host targets of SidC/SdcA ligase activity have been found (see Discussion for Chapter 2). An unintentional discovery may provide a clue as to how the SidC family could regulate ubiquitination indirectly during infection. *L.p.* secretes a class of effectors, known as metaeffectors, that regulate the activity of other bacterial effectors during infection. These effectors allow *L.p.* to dynamically control proteins outside of its cell body that might be excessively toxic to the host, or trap *L.p.* in an early stage of LCV maturation. Many metaeffectors have now been identified, including LubX, which ubiquitinates SidH, resulting in its proteasomal degradation[82]; SidJ, which glutamylates SidE family members to disrupt activity and LCV localization[87,88], and MesI, which suppresses the potent translation inhibitor SidI[89].

In an early attempt to determine if other effectors beyond SidC/SdcA contributed to Rab5 ubiquitination during infection, we turned to a previously generated strain known as the pentuple mutant, which lacks about 20% of identified bacterial effectors[16]. Importantly, these missing effectors include SidC/SdcA, so we decided to test whether complementation of the pentuple strain with plasmid encoded SdcA was sufficient to rescue Rab5 ubiquitination. Much to our surprise, we found that Rab5 monoubiquitination, while weaker than in WT infection, was still robust during pentuple infection (**Fig 4.3A**). To ensure that our pentuple strain truly lacks SidC/SdcA, we performed a series of colony PCRs using primers that bind within the SidC and
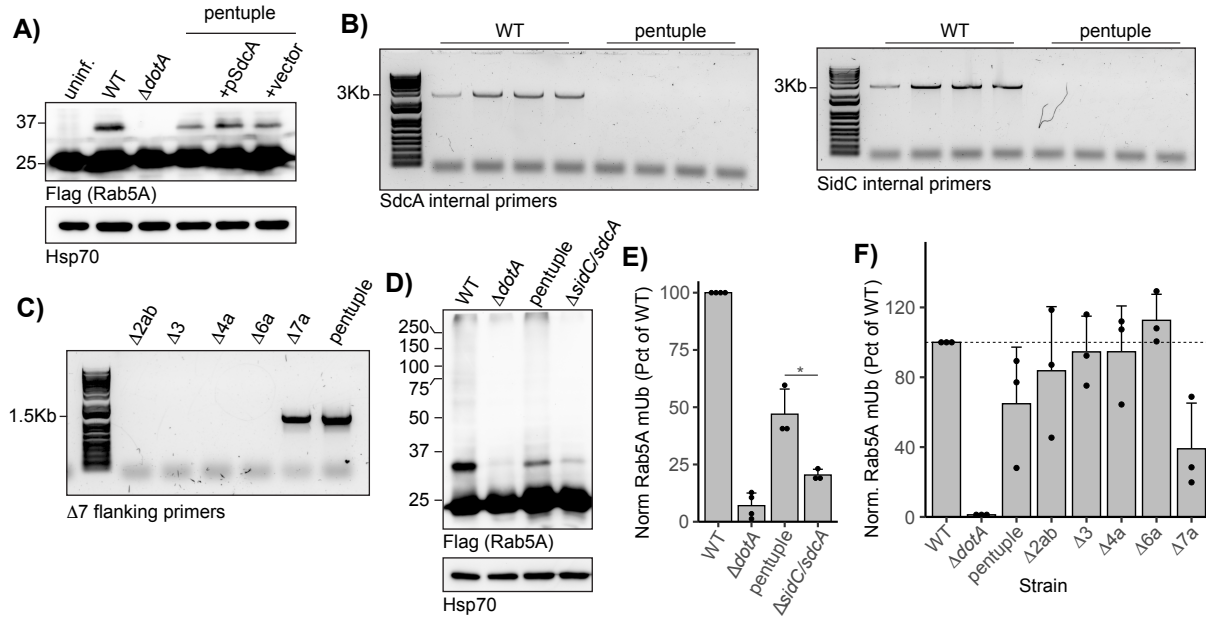
Figure 4.3 The pentuple strain ubiquitinates Rab5 without SidC/SdcA.

(A) Immunoblot analysis of Flag Rab5A monoubiquitination in 293T FcγR cells infected with indicated *L.p.* strain for 4 hours. **(B)** DNA gel analysis of colony PCR products for SdcA and SidC in *L.p.* WT and pentuple. Expected size for WT gene ~2700 bp for both genes. **(C)** DNA gel analysis of colony PCR products for 7a region flanking primers. Expected size for 7a deletion strain ~700-1500 bp, WT locus ~80kb. **(D)** Immunoblot analysis of Flag Rab5A ubiquitination in 293T FcγR cells infected with indicated *L.p.* strain for 4 hours (MOI=20). **(E)** Normalized Rab5A monoubiquitination intensity was calculated as a percentage of *L.p.* WT infection levels (see Methods), (N=3) for experiments described in (D). Data was subjected to ANOVA and Tukey-Kramer post-hoc test, * =$p<0.05$. **(F)** Quantification of monoubiquitination of Rab5A during infection with the indicated strain as in (E).

SdcA sequences, as well as pair hybridizing to the flanking region of the genomic island deletion that spans SidC/SdcA. The pentuple strain lacks five genomic regions - 2ab, 3, 4a, 6a, and 7a; SidC/SdcA reside within region 7a. No product was produced for the SidC/SdcA primers for the pentuple strain (**Fig 4.3B**), while a clear band was produced for the genomic island flanking reaction for both the d7a and pentuple strains (**Fig 4.3C**). Note that the WT 7a locus present in d2ab, d3, d4a, and d6a is too large (~80 kilobases) to amplify with our experimental setup. To directly compare the pentuple strain to a strain lacking only SidC/SdcA, we infected cells expressing Flag Rab5 with *L.p.* WT, Δ*dotA*, pentuple, and Δ*sidC/sdcA*, and assessed Rab5

ubiquitination efficiency (**Fig 4.3D-E**). Consistently, we see stronger ubiquitination of Rab5 during pentuple infection compared to the Δ*sidC/sdcA* strain. While we can only roughly assess Rab5 ubiquitination efficiency by our Western blot quantification strategy, we decided to examine whether any one island deletion strain had much higher Rab5 ubiquitination efficiency than the WT strain, as this could explain the pentuple phenotype. We do not observe strong increases in Rab5A monoubiquitination for any of the individual genomic island deletions and found that the Δ7a strain has ubiquitination efficiency similar to the SidC/SdcA knockout strain (**Fig 4F**). This finding is consistent with a model in which SidC/SdcA inhibit an effector that is a negative regulator of Rab5 ubiquitination that is present in one of the deleted genomic regions in the pentuple strain outside of region 7a.

Discussion

In Chapter 4, we describe a burst of ubiquitination activity during early *L.p.* infection modifying both host and bacterial substrates. We find that the effectors SidC/SdcA are required for this burst, an interesting observation given that SidC/SdcA are also required for ubiquitin recruitment to the LCV during early infection[47]. We discover that the *L.p.* pentuple strain, lacking SidC/SdcA and about 70 other effectors, induces stronger ubiquitination of Rab5A than a SidC/SdcA knockout alone. This data is consistent with a model in which SidC/SdcA negatively regulate an effector that antagonizes the ubiquitination of Rab5A, rather than ubiquitinating Rab5A directly. This hypothesis posits that SidC/SdcA are metaeffectors, modulating the activity of other bacterial effectors during infection. This model could explain the difficulty multiple groups have experienced in trying to find a target of SidC/SdcA ligase activity while ectopically expressing SidC/SdcA[46,70]. Further experimentation testing this hypothesis is warranted, as defining a molecular mechanism for these enigmatic effectors will vastly improve our understanding of how and why *L.p.* builds a ubiquitin coat around its vacuole.

MATERIALS AND METHODS

Cell Lines

HEK293T cells (female), HEK293 cells (female) stably expressing the Fcγ receptor IIb (HEK293 FcγR cells), and HeLa FcγR cells were cultured in Dulbecco's Modified Eagle's Medium (DMEM, GIBCO) containing 10% fetal bovine serum (FBS, VWR) at 37°C and 5% CO_2. FcγR expressing cell lines were gifts from the lab of Dr. Craig Roy at Yale University. U937 cells (a gift from Dr. Michael Bassik at Stanford University) were cultured in RPMI-1640 (Corning) supplemented with 10% heat-inactivated FBS (VWR). U937 were differentiated into macrophage-like cells in 20 ng/mL phorbol 12-myristate 13-acetate (PMA, Sigma) for 72 hours, then re-plated in media without PMA and allowed to rest for 48 hours before *L.p* infection.

Bacterial Strains and Plasmids

Experiments were performed with *Legionella pneumophila* serogroup 1, strain Lp01 or Lp02. Avirulent T4SS-null strains were derived as previously described[90,91]. *L. pneumophila* strains were grown on Charcoal Yeast Extract (CYE) agar plates or AYE broth supplemented with ($FeNO_3$ 0.135g/10mL) and cysteine (0.4g/10mL). Growth media for Lp02 thymidine auxotroph-derived strains was supplemented with 100 ug/mL thymidine. For strains carrying complementation plasmids, chloramphenicol (5 µg/mL) was supplemented for plasmid maintenance, and IPTG (1 mM) was added for 2 hours of induction prior to infection. The unmarked gene deletion Δ*sidC-sdcA* strain was derived from the parental strain using allelic exchange as described previously[91]. Rab5A, Rab5B, and Rab5C coding sequences were amplified from HeLa cDNA and cloned into a pcDNA3.1 mammalian expression vector containing the appropriate N-terminal tag (3XFlag or mCherry). Rab5A, Rab1A, and Rab10 CAAX deletion inserts were derived from appropriate full-length plasmid by PCR amplification of the desired region.

Infection of Cultured Mammalian Cells with *L.p.*

Infections with *L.p.* were performed as previously described (Treacy-Abarca and Mukherjee, 2015). *L.p.* heavy patches grown for 48 h on CYE plates were either used directly for infection, or for overnight liquid cultures in AYE medium until reaching an OD600 of 3. *L.p.* from the overnight culture was enumerated and the appropriate amount was opsonized with *L.p.*-specific antibodies at a dilution of 1:2000 in cell growth medium for 20 min. HEK293 FcγR were grown on poly-lysine coated cell culture plates to a confluency of 80% and infected with the *L.p.* WT strain or the isogenic Δ*dotA* mutant strain at a multiplicity of infection (MOI) of 1-100 as indicated. The infection was synchronized by centrifugation of the plates at 1000xg for 5 min. To prevent internalization of any remaining extracellular bacteria at later timepoints, cells were washed three times with warm PBS after 1 h of infection and fresh growth medium was added. Cells were collected for down-stream processing at the indicated timepoints. Uninfected samples used as controls for infection experiments were mock-infected using media and opsonization antibody only.

Sample Preparation for Proteomics Analysis

HEK293 FcγR infected for 1 h or 8 h with the *L.p.* WT strain Lp01 or the isogenic Δ*dotA* mutant were infected at an MOI of 100. Uninfected HEK293 FcγR cells were included as a control. Cells were washed with ice-cold PBS, collected and the pellet was frozen at -80°C. Cell pellets were lysed by probe sonication in three pulses of 20% amplitude for 15 s in a lysis buffer consisting of: 8 M urea, 150 mM NaCl, 100 mM ammonium bicarbonate, pH 8; added per 10 ml of buffer: 1 tablet of Roche mini-complete protease inhibitor EDTA free and 1 tablet of Roche PhosSTOP. In order to remove insoluble precipitate, lysates were centrifuged at 16,100 g at 4°C for 30 min. A Bradford Assay (Thermo) was performed to measure protein concentration in cell lysate supernatants. 6 mg of each clarified lysate was reduced with 4 mM tris(2-

carboxyethyl)phosphine for 30 min at room temperature and alkylated with 10 mM iodoacetamide for 30 min at room temperature in the dark. Remaining alkylated agent was quenched with 10 mM 1,4-dithiothreitol for 30 min at room temperature in the dark. The samples were diluted with three starting volumes of 100 mM ammonium bicarbonate, pH 8.0, to reduce the urea concentration to 2 M. Samples were incubated with 50 µg of sequencing grade modified trypsin (Promega) and incubated at room temperature with rotation for 18 hr. The sample pH was reduced to approximately 2.0 by the addition of 10% trifluoroacetic acid (TFA) to a final concentration of 0.3% trifluoroacetic acid. Insoluble material was removed by centrifugation at 16,000 g for 10 min. Peptides were desalted using SepPak C18 solid-phase extraction cartridges (Waters). The columns were activated with 1 ml of 80% acetonitrile (I), 0.1% TFA, and equilibrated 3 times with 1 ml of 0.1% TFA. Peptide samples were applied to the columns, and the columns were washed 3 times with 1 ml of 0.1% TFA. Peptides were eluted with 1.2 ml of 50% I, 0.25% formic acid. Peptides were divided for global protein analysis (10 µg) or diGly-enrichment (remaining sample), and lyophilized.

diGlycine Peptide Enrichment by Immunoprecipitation

Peptide samples were subjected to ubiquitin remnant immunoaffinity. 10 uL of PTMScan® Ubiquitin Remnant Motif (K-ε-GG) Antibody Bead Conjugate purification (Cell Signaling) slurry was used per 1 mg peptide sample. Ubiquitin remnant beads were washed twice with IAP buffer, then split into individual 1.7 mL low bind tubes (Eppendorf) for binding with peptides. Peptides were dried with a centrifugal evaporator for 12 hours to remove TFA in the elution. The lyophilized peptides were resuspended in 1 ml of IAP buffer (50 mM 4- morpholinepropnesulfonic acid, 10 mM disodium hydrogen phosphate, 50 mM sodium chloride, pH 7.5). Peptides were sonicated and centrifuged for 5 minutes at 16,100g. The soluble peptide supernatant was incubated with the beads at 4˚C for 90 minutes with rotation. Unbound peptides were separated from the beads after centrifugation at 700g for 60 seconds. Beads containing peptides with di-glycine remnants

were washed twice with 500 μL of IAP buffer, then washed twice with 500 μL of water, with a 700g 60s centrifugation to allow the collection of each wash step. Peptides were eluted twice with 60 μL of 0.15% TFA. Di-glycine remnant peptides were desalted with UltraMicroSpin C18 column (The Nest Group). Desalted peptides were dried with a centrifugal adaptor and stored at -20°C until analysis by liquid chromatograph and mass spectrometry.

Mass Spectrometry Data Acquisition and Processing

Samples were resuspended in 4% formic acid, 4% acetonitrile solution, separated by a reversed-phase gradient over a nanoflow column (360 μm O.D. x 75 μm I.D.) packed with 25 cm of 1.8 μm Reprosil C18 particles with (Dr. Maisch), and directly injected into an Orbitrap Fusion Lumos Tribrid Mass Spectrometer (Thermo). Total acquisition times were 120 min for protein abundance, 100 min for phosphorylation, and 70 min for ubiquitylation analyses. Specific data acquisition settings are detailed in Ref #X, Supplemental table 1. Raw mass spectrometry data were searched with MaxQuant against both the human proteome (UniProt canonical protein sequences downloaded January 11, 2016) and the *Legionella Pneumophila Philadelphia* proteome (downloaded July 17, 2017). Peptides, proteins, and PTMs were filtered to 1% false discovery rate in MaxQuant[92]. Statistical analysis of quantifications obtained from MaxQuant was performed with the artMS Bioconductor package (version 0.9) (see Key Resources table). Each dataset (proteome and ubiquitinome) was analyzed independently. Quality control plots were generated using the artMS quality control functions. The site-specific relative quantification of posttranslational modifications required a preliminary step consisting of providing the ptm-site/peptide-specific annotation ("artmsProtein2SiteConversion()" function). artMS performs the relative quantification using the MSstats Bioconductor package (version 3.14.1)[93]. Contaminants and decoy hits were removed. Samples were normalized across fractions by median-centering the Log_2-transformed MS1 intensity distributions. Imputation strategy: Log2FC for protein/sites with missing values in one condition but found in ≥ 2 biological replicates of the other condition of

any given comparison were estimated by imputing intensity values from the lowest observed MS1-intensity across sample peptides[94]; p-values were randomly assigned between 0.05 and 0.01 for illustration purposes.

Cell Lysis, Immunoprecipitation, and Immunoblot Analysis

HEK293 FcγR cells grown on poly-lysine coated plates were treated as indicated, washed three times with ice-cold PBS and harvested with a cell scraper. Cells were pelleted at 3000xg for 10 minutes at 4C. For preparation of whole cell lysates, cell pellets were resuspended in RIPA buffer supplemented with cOmplete Protease Inhibitor Cocktail (Roche), phenymethylsulphonyl fluoride (PMSF, 1 mM), and N-ethylmaleimide (NEM, 10 mM) and lysed under constant agitation for 20 min at 4°C. Cell debris was removed by centrifugation at 16,000xg for 20 min at 4°C. Protein concentration was measured using the Pierce 660nm Protein Assay Kit or the Pierce™ BCA Protein Assay Kit (Thermo Fisher Scientific). For each sample, 20-30 µg of proteins were denatured in SDS sample buffer/5% β-mercaptoethanol at 95°C for 5 min. For Flag pulldown assays, cells were lysed in 137 mM NaCl, 20 mM Tris base pH 8, 1% v/v NP40, 2 mM EDTA supplemented with inhibitors as above. Protein concentrations were measured as above, and lysates were diluted to equal volumes at equal concentrations (1-3 mg/mL). Input samples were removed and prepared for SDS-PAGE as above. Anti-Flag M2 antibody was added at a 1:50 dilution to the remaining lysate and rotated overnight at 4C. Samples were incubated with rotation with Invitrogen Dynabeads Protein G (1.5 mg/sample) for 2 hours at 4C. Beads were washed three times with ice cold lysis buffer, and bound proteins were eluted in 30 uL 2X SDS sample buffer for 10 minutes at 95C. For ubiquitin pulldown assays using the SignalSeeker kit (Cytoskeleton Inc), cells were lysed in provided BlastR buffer with protease inhibitor and NEM, and total protein concentration measured using Precision Red Advanced protein assay. Lysates were diluted to 1 mg/mL, and 1 mL of diluted lysate was incubated with either unconjugated (control) or ubiquitin binding domain conjugated beads for 2 hours at 4C on a rotating platform.

Beads were washed three times in wash buffer, and bound proteins were eluted using kit spin columns. For immunoblot analysis, samples were loaded on 8-12% SDS-polyacrylamide gels and separated by SDS-PAGE. Proteins were transferred to PVDF membranes (0.45 µm, Millipore) at 30 V, 4°C for 16 h. For total ubiquitin blots, total protein was quantified before blocking using Invitrogen No-Stain Protein Labeling Reagent. Membranes were washed with PBS-T (PBS/ 0.1% Tween-20 (Thermo Fisher Scientific)), blocked with 5% Blotting Grade Blocker Non Fat Dry Milk (Bio-Rad) for 1 h at room temperature and incubated with the primary antibodies diluted in blocking buffer/0.02% (w/v) sodium azide overnight at 4°C. Membranes were washed three times with PBS-T and incubated with Goat Anti-Mouse IgG (H+L) HRP Conjugate (Thermo Fisher Scientific), Goat Anti-Rabbit IgG (H+L) (Thermo Fisher Scientific), HRP Conjugate, diluted at 1:5000 in blocking buffer for 60 min at room temperature. After three washes with PBS-T, membranes were incubated with Amersham ECL Western Blotting Detection Reagent (Global Life Science Solutions) for 1 min and imaged on a ChemiDoc Imaging System (BioRad).

Cellular Fractionation

After indicated treatment, cells were collected by gentle scraping into the culture medium and pelleted at 200xg for 5 minutes at 4C. Cells were washed in ice cold 1X PBS, then gently homogenized in ice cold homogenization buffer (150 mM KCl, 20 mM HEPES pH 7.4, 2 mM EDTA, 1X cOmplete Protease Inhibitor Cocktail). Cells were lysed with 20-30 passes through a 25g needle. Lysates were spun at 0.6xg, 4C for 5 minutes to remove nuclei and unlysed cells. Post-nuclear supernatant was spun at 150,000xg for 45 minutes, and the supernatant transferred to a new tube (cytosolic fraction). The membrane pellet was washed once in homogenization buffer and re-pelleted at 150,000xg, 4C for 20 minutes. The supernatant was removed, and the membrane pellet resuspended in homogenization buffer + 1% v/v Triton-X 100.

Immunoblot Quantification

Images were exported from ImageLab (BioRad) as 16-bit tiff and analyzed in ImageJ. Plot profiles were generated for each lane and the integrated density was calculated using the ImageJ built in gel analyzer tools. Total ubiquitin signal was normalized to total protein, and the fold change was calculated compared to the appropriate uninfected control. To calculate normalized Rab monoubiquitination intensity, integrated density was measured for the unmodified band at sub-saturated exposure. Integrated density was measured for the higher molecular weight monoubiquitination band at the lowest exposure in which this band was visible. Normalized Rab monoubiquitination was calculated as follows: IntDen monoUb/(IntDen monoUb + InDen unmod Ub). To standardize these values across biological replicates, values are represented as a percentage of the WT infection condition for each replicate. The intensity profiles in Fig 1.5B were generated in Fiji.

Immunofluorescence and Image Acquisition

HeLa FcγR cells were grown on poly-lysine coated coverslips in 24well cell culture plates. Cells were treated as indicated, washed three times with PBS and fixed in 4% paraformaldehyde/PBS for 15 min at room temperature. For standard gentle permeabilization, cells were then treated with 2% BSA, 0.5% saponin in PBS (blocking/permeabilization buffer) for 1h at RT. For harsh 5% SDS permeabilization, cells were incubated in 5% SDS in potassium free 1X TBS for one hour at RT on an orbital shaker, and then blocked for 1 hour in 2% BSA in PBS at RT. Cells were stained with primary antibodies diluted in blocking or blocking/permeabilization buffer overnight at 4C, washed three times with PBS and stained with secondary antibodies diluted in blocking or blocking/permeabilization buffer for 1h at RT. Cells were then stained with Hoechst33342 at 1:2000 in PBS for 10 min and washed three times with PBS. Coverslips were dipped three times into purified ddH$_2$O to remove salts, dried and mounted on microscopy glass slides with Prolong Diamond antifade 5 (Thermo Fisher Scientific). Slides were cured overnight

at room temperature. Images were acquired on a Nikon Ti2 Eclipse inverted microscope outfitted with a CREST X-Light V2 spinning disk unit and Photometrics Prime 95B CMOS camera (no binning, 16-bit). All images were acquired using a 60X 1.4NA oil immersion objective. NIS-Elements Advanced Research software was used to control the microscope and acquire images. Lasers were used at the following intensities: ExW 365nm 25%, ExW 488nm 25%, ExW 561nm 100%, ExW 640nm 100%. Exposure time ranged from 10-50 ms. Experimental conditions were blinded either before image acquisition, or before image analysis using the Fiji Blind Analysis Tools plugin filename encrypter.

Image Analysis

For manual LCV scoring, max intensity Z projections were generated. LCVs were scored positive if the LCV region was visible in the protein marker of interest channel only (i.e. without the *L.p.* marker). LCV area measurements in Figure 2.1 were carried out in Fiji using the freehand selection tool. For CellProfiler analysis, regions of interest were cropped from max intensity Z projections and background subtracted (rolling ball radius = 5-10 px) in Fiji. Anti-*Legionella* antibody positive regions were used to generate primary LCV objects. For Rab5 and ubiquitin positive region area analysis, secondary objects were generated from the LCV primary objects. Size/shape measurements were made for both the primary LCV and secondary Rab5/Ub object. Only Rab5/Ub positive LCVs were included in this analysis. For CTLF measurements, a tertiary object was generated by subtracting a +5px expansion of the LCV primary object from a +10 expansion of the LCV primary object. Object intensity was then measured in the Rab5 channel for both the primary LCV and the tertiary background object. Object size/shape was also measured for the LCV primary object. All LCVs associated with host cells were included in this analysis. For endosome size analysis, regions enclosing transfected uninfected cells in the Δ*dotA* infected condition images were cropped and background subtracted (rolling ball radius = 5 px). Rab5 signal was used to generate primary objects, which were then analyzed by the

MeasureObjectSizeShape module. Whole cell CTCF measurements were done in Fiji using the freehand selection tool to approximate cell outlines. Representative images in all figures are max intensity Z projections.

Transfections

All transfections were performed with jetPRIME (Polyplus). HEK293 FcγR or HeLa FcγR cells were grown to 60% confluency and transfected according to the manufacturer's recommendations. For transfection of plasmid DNA, 0.25 µg DNA was used for 24well plates, 1-2 µg DNA for 6 well plates, 2-3 ug for 60 mm plates, and 5-10 ug for 100 mm plates. 24h after transfection, cells were treated as indicated and analyzed or harvested. For experiments in which HA-ubiquitin was transiently co-expressed, the expression construct was added at 20% of the total amount of DNA to minimize pleiotropic effects of strong ubiquitin overexpression.

Colony Screen PCR and Gel Electrophoresis

Single *L.p.* colonies were suspended in 50 uL sterile milliQ water. 1.5 uL of cell suspension was added to 20 uL 1X GoTaq Green master mix plus each primer at 0.5 uM in nuclease free water. Reactions were run in a BioRad thermocycler as follow: 3 min 98C, then 10s 98C, 30s annealing at variable temp, 1-3 min extension 72C for 25 cycles, followed by a final extension at 72C for 5 minutes. 10 uL product was run on a 1% agarose gel in TAE stained with SybrSafe (Invitrogen) alongside 1kb+ ladder (Invitrogen) for 25 minutes at 120V and imaged on a ChemiDoc imaging system (BioRad).

Statistical Analysis and Data Representation

Plots were generated in R using the ggplot2 package. All bar graphs represent the mean value across biological replicates, and individual values for each replicate are shown for N<10. Jitter plots are colored coded by biological replicate and show individual measurements (small

dots), mean for each biological replicate (large dots), and the mean for all combined data (bar). Individual points in line graphs represent mean values across biological replicates. Error bars on bar and line graphs represent standard deviation. For all Western blot quantification, CTLF and multi-condition LCV morphology measurements, data were subjected to a one-way ANOVA followed by a Tukey-Kramer post-hoc test for each pair of means (* = $p<0.05$, n.s. = $p\geq0.05$). For CTCF and two condition morphology measurements, data were subjected to a Welch's t-test (n.s. = $p\geq0.05$, * = $p<0.05$, ** = $p<0.005$). For LCV scoring, G test of independence was performed on pooled counts for each nominal measurement variable (positive vs. negative, or replication bin) and experimental condition from all biological replicates. Upon verifying significance ($p<0.05$), data from experiments with more than two conditions (e.g. multiple strains) was subjected to pairwise comparisons between conditions by post-hoc G-test using a Bonferroni-adjusted p-value as a significance threshold as indicated in figure legend. For all G tests, n.s. = $p\geq$ threshold, * = $p<$ threshold, ** = $p<$threshold$\times10^{-1}$, *** = $p<$ threshold$\times10^{-2}$.

Data Availability

The mass spectrometry data files have been deposited to the ProteomeXchange Consortium (http://proteomecentral.proteomexchange.org) via the PRIDE partner repository with the dataset identifier PXD019217[95].

Table 1: Key resources

Cell lines		
Cell Line	**ID**	**Source**
Human: HEK293 cells stably expressing FcγRIIb	derived from ATCC CRL-1573	Gift from Dr. Craig Roy
Human: HEK293T cells stably expressing FcγRIIb	derived from ATCC CRL-3216	This study
Human: HeLa cells stably expressing FcγRIIb	derived from ATCC CCL-2	Gift from Dr. Craig Roy
Human: U937	ATCC CRL-1593.2	Gift from Dr. Michael Bassik
Bacterial Strains		
Strain	**ID**	**Source**
Legionella pneumophila serogroup 1 strain Lp01	LEG001	Gift from Dr. Craig Roy[91]
Lp01 Δ*dotA*	LEG002	Gift from Dr. Craig Roy[91]
Lp01 Δ*sidC/sdcA* (Δ*lpg2510-2511)*	LEG073	Gift from Dr. Craig Roy
Lp01 Δ*sidC/sdcA* pJB1806	LEG184	This study
Lp01 Δ*sidC/sdcA* pJB1806::SdcA	LEG081	This study
Lp01 Δ*sidC/sdcA* pJB1806::SidC	LEG082	This study
Legionella pneumophila serogroup 1 strain Lp02 *rpsL hsdR thyA*	LEG003	Gift from Dr. Craig Roy[90]
Lp02 Δ*dotA* (LP03)	LEG004	Gift from Dr. Craig Roy[90]
Lp02 Δ*sidC/sdcA* (Δ*lpg2510-2511)*	LEG173	This study
Lp02 Δ*sidC/sdcA* pJB1806	LEG179	This study

Bacterial Strains, continued		
Strain	**ID**	**Source**
Lp02 Δ*sidC/sdcA* pJB1806::SdcA	LEG180	This study
Lp02 Δ*sidC/sdcA* pJB1806::SidC	LEG181	This study
Lp02 Δ*sidE* Δ*sdeC* Δ*sdeBA* (Δ*lpg0234*, Δ*lpg2153* Δ*lpg2156-2157*), annotated as "Δ*sidE/sdeABC*" for brevity	LEG151	Gift from Dr. Ralph Isberg[88]
Lp02 Δ*sidE* Δ*sdeC* Δ*sdeBA* pJB1806	LEG170	This study
Lp02 Δ*sidE* Δ*sdeC* Δ*sdeBA* pJB1806::SdeB	LEG171	This study
Colony PCR primer sequences		
Name	**Sequence**	**Source**
SdcA F	TCACACAGGAAACAGAATTC GTGATGAACATGGTTGACAA AATAAAATTC	This study
SdcA R	GCCTGCAGGTCGACTCTAGA CTATATTGTATTCCTAACAGT TTCTCTGAG	This study
SidC F	TCACACAGGAAACAGAATTC ATGGTGATAAACATGGTTGA CGTA	This study
SidC R	GCCTGCAGGTCGACTCTAGA CTATTTCTTTATAATTCCCGT GTACAAAGT	This study
7a flank F	TGTGCTCGTCTCTTCAGGC	This study
7a flank R	AACAGTTCCTCGATTTCAACG AATAGAA	This study
Recombinant DNA		
Description	**ID**	**Source**
pcDNA3.1 mCherry-Rab5A	pAS042	This study
pcDNA3.1 mCherry-Rab5A Δ*CAAX*	pAS049	This study

Recombinant DNA, continued		
Description	**ID**	**Source**
pcDNA3.1 3XFlag-Rab5A	pAS034	This study
pcDNA3.1 3XFlag-Rab5A ΔCAAX	pAS041	This study
pcDNA3.1 3XFlag-Rab5B	pAS050	This study
pcDNA3.1 3XFlag-Rab5C	pAS051	This study
pEGFP-C2	pSM150	Gift from Dr. Craig Roy
pEGFP-C2 GFP-SdcA	pSM261	Gift from Dr. Craig Roy
pEGFP-C2 GFP-SidC	pSM174	Gift from Dr. Craig Roy
pRK5-HA Ubiquitin	pSM099	Gift from Dr. Kohei Arasaki
Antibodies		
Antigen	**Dilution (application)**	**Source**
Rab5A	1:1000 (WB), 1:200 (IF)	Cell Signaling Technology (46449)
EEA1	1:100 (IF)	Abcam (ab70521)
Lamp1	1:200 (IF)	Cell Signaling Technology (15665)
Flag	1:2500 (WB), 1:50 (IP)	Sigma (F1804)
Flag (HRP conjugate)	1:2500 (WB)	Sigma (A8592)
Hsp70	1:2000 (WB)	Santa Cruz (sc-66048)
GFP	1:1000 (WB)	Roche (11814460001)
Ubiquitin	1:1000 (WB)	Cell Signaling Technology (3933S)
Conjugated ubiquitin FK2	1:200 (IF)	Sigma (ST1200)
HA (HRP conjugate)	1:1000 (WB)	Thermo (26183-HRP)
L. pneumophila	1:2000 (opsonization)	Thermo (PA1-7227)

Antibodies, continued		
Antigen	**Dilution (application)**	**Source**
Goat anti-Rabbit IgG (H+L) Highly Cross-Adsorbed Secondary Antibody (Alexa Fluor 633)	1:500 (IF)	Life Technologies (a21071)
Goat anti-Mouse IgG (H+L) Highly Cross-Adsorbed Secondary Antibody (Alexa Fluor 488)	1:500 (IF)	Life Technologies (a11029)
Goat Anti-Mouse IgG (H+L) HRP Conjugate	1:5000 (WB)	Life Technologies (A16066)
Goat Anti-Rabbit IgG (H+L) HRP Conjugate	1:5000 (WB)	Life Technologies (A16096)
Mouse Anti rabbit IgG (Conformation Specific) - HRP conjugate	1:2000 (WB) - used for ubiquitin immunoblots to avoid detection of opsonization antibody	Cell Signaling Technology (5127S)
Kits		
Signal-Seeker™ Ubiquitination Detection Kit	Cytoskeleton, Inc.	Cat.# BK161
Software and algorithms		
Name	**Source**	**Link**
MaxQuant	Ref. 92	https://www.maxquant.org
artMS Bioconductor package (v 0.9)		https://bioconductor.org/packages/release/bioc/html/artMS.html
factoextra R package		https://zenodo.org/record/8093247
DeepVenn	Ref. 96	https://www.deepvenn.com
Jalview	Ref. 97	https://www.jalview.org
Fiji	Ref. 98	https://fiji.sc
ggplot2 (R package for generating plots)		https://ggplot2.tidyverse.org
CellProfiler	Ref. 99	https://cellprofiler.org/

Deposited data		
Raw data from mass spectrometry	ProteomeXchange Consortium (http://proteomecentral.proteomexchange.org) via PRIDE partner repository	PXD019217

REFERENCES

1. Langemeyer, L., Fröhlich, F., and Ungermann, C. (2018). Rab GTPase Function in Endosome and Lysosome Biogenesis. Trends Cell Biol. *28*, 957–970. 10.1016/j.tcb.2018.06.007.

2. Case, E.D.R., and Samuel, J.E. (2016). Contrasting Lifestyles Within the Host Cell. Microbiol. Spectr. *4*. 10.1128/microbiolspec.vmbf-0014-2015.

3. Moffatt, J.H., Newton, P., and Newton, H.J. (2015). Intracellular replication of Coxiella. Cell. Microbiol. *17*, 621–631. 10.1111/cmi.12432.

4. Horwitz, M.A. (1983). Formation of a novel phagosome by the Legionnaires' disease bacterium (Legionella pneumophila) in human monocytes. J. Exp. Med. *158*, 1319–1331. 10.1084/jem.158.4.1319.

5. Horwitz, M.A. (1983). The Legionnaires' disease bacterium (Legionella pneumophila) inhibits phagosome-lysosome fusion in human monocytes. J. Exp. Med. *158*, 2108–2126. 10.1084/jem.158.6.2108.

6. Vogel, Joseph.P., Andrews, H.L., Wong, S.K., and Isberg, R.R. (1998). Conjugative Transfer by the Virulence System of Legionella pneumophila. Science *279*, 873–876. 10.1126/science.279.5352.873.

7. Noack, J., and Mukherjee, S. (2020). "Make way": Pathogen exploitation of membrane traffic. Curr. Opin. Cell Biol. *65*, 78–85. 10.1016/j.ceb.2020.02.011.

8. Sherwood, R.K., and Roy, C.R. (2016). Autophagy Evasion and Endoplasmic Reticulum Subversion: The Yin and Yang of Legionella Intracellular Infection. Annu. Rev. Microbiol. *70*, 413–433. 10.1146/annurev-micro-102215-095557.

9. Choy, A., Dancourt, J., Mugo, B., O'Connor, T.J., Isberg, R.R., Melia, T.J., and Roy, C.R. (2012). The Legionella Effector RavZ Inhibits Host Autophagy Through Irreversible Atg8 Deconjugation. Science *338*, 1072–1076. 10.1126/science.1227026.

10. Rolando, M., Sanulli, S., Rusniok, C., Gomez-Valero, L., Bertholet, C., Sahr, T., Margueron, R., and Buchrieser, C. (2013). Legionella pneumophila Effector RomA Uniquely Modifies Host Chromatin to Repress Gene Expression and Promote Intracellular Bacterial Replication. Cell Host Microbe *13*, 395–405. 10.1016/j.chom.2013.03.004.

11. Belyi, Y., Tabakova, I., Stahl, M., and Aktories, K. (2008). Lgt: a Family of Cytotoxic Glucosyltransferases Produced by Legionella pneumophila. J. Bacteriol. *190*, 3026–3035. 10.1128/jb.01798-07.

12. Subramanian, A., Wang, L., Moss, T., Voorhies, M., Sangwan, S., Stevenson, E., Pulido, E.H., Kwok, S., Chalkley, R.J., Li, K.H., et al. (2023). A Legionella toxin exhibits tRNA mimicry and glycosyl transferase activity to target the translation machinery and trigger a ribotoxic stress response. Nat. Cell Biol. *25*, 1600–1615. 10.1038/s41556-023-01248-z.

13. Moss, S.M., Taylor, I.R., Ruggero, D., Gestwicki, J.E., Shokat, K.M., and Mukherjee, S. (2019). A Legionella pneumophila Kinase Phosphorylates the Hsp70 Chaperone Family to Inhibit Eukaryotic Protein Synthesis. Cell Host Microbe *25*, 454-462.e6. 10.1016/j.chom.2019.01.006.

14. Best, A., and Kwaik, Y.A. (2018). Evolution of the Arsenal of Legionella pneumophila Effectors To Modulate Protist Hosts. mBio *9*, e01313-18. 10.1128/mbio.01313-18.

15. Roy, C.R., Berger, K.H., and Isberg, R.R. (1998). Legionella pneumophila DotA protein is required for early phagosome trafficking decisions that occur within minutes of bacterial uptake. Mol. Microbiol. *28*, 663–674. 10.1046/j.1365-2958.1998.00841.x.

16. O'Connor, T.J., Adepoju, Y., Boyd, D., and Isberg, R.R. (2011). Minimization of the Legionella pneumophila genome reveals chromosomal regions involved in host range expansion. Proc. Natl. Acad. Sci. *108*, 14733–14740. 10.1073/pnas.1111678108.

17. Huotari, J., and Helenius, A. (2011). Endosome maturation. EMBO J. *30*, 3481–3500. 10.1038/emboj.2011.286.

18. Kotewicz, K.M., Ramabhadran, V., Sjoblom, N., Vogel, J.P., Haenssler, E., Zhang, M., Behringer, J., Scheck, R.A., and Isberg, R.R. (2017). A Single Legionella Effector Catalyzes a Multistep Ubiquitination Pathway to Rearrange Tubular Endoplasmic Reticulum for Replication. Cell Host Microbe *21*, 169–181. 10.1016/j.chom.2016.12.007.

19. Cherfils, J., and Zeghouf, M. (2013). Regulation of Small GTPases by GEFs, GAPs, and GDIs. Physiol. Rev. *93*, 269–309. 10.1152/physrev.00003.2012.

20. Poteryaev, D., Datta, S., Ackema, K., Zerial, M., and Spang, A. (2010). Identification of the Switch in Early-to-Late Endosome Transition. Cell *141*, 497–508. 10.1016/j.cell.2010.03.011.

21. Lawrence, G., Brown, C.C., Flood, B.A., Karunakaran, S., Cabrera, M., Nordmann, M., Ungermann, C., and Fratti, R.A. (2014). Dynamic association of the PI3P-interacting Mon1-Ccz1 GEF with vacuoles is controlled through its phosphorylation by the type 1 casein kinase Yck3. Mol. Biol. Cell *25*, 1608–1619. 10.1091/mbc.e13-08-0460.

22. Falkenburger, B.H., Jensen, J.B., Dickson, E.J., Suh, B., and Hille, B. (2010). SYMPOSIUM REVIEW: Phosphoinositides: lipid regulators of membrane proteins. J. Physiol. *588*, 3179–3185. 10.1113/jphysiol.2010.192153.

23. Sturgill-Koszycki, S., and Swanson, M.S. (2000). Legionella pneumophila Replication Vacuoles Mature into Acidic, Endocytic Organelles. J. Exp. Med. *192*, 1261–1272. 10.1084/jem.192.9.1261.

24. Weber, S., Wagner, M., and Hilbi, H. (2014). Live-Cell Imaging of Phosphoinositide Dynamics and Membrane Architecture during Legionella Infection. mBio *5*, e00839-13. 10.1128/mbio.00839-13.

25. Li, G., Liu, H., Luo, Z., and Qiu, J. (2021). Modulation of phagosome phosphoinositide dynamics by a Legionella phosphoinositide 3-kinase. EMBO Rep. *22*, e51163. 10.15252/embr.202051163.

26. Weber, S.S., Ragaz, C., Reus, K., Nyfeler, Y., and Hilbi, H. (2006). Legionella pneumophila Exploits PI(4)P to Anchor Secreted Effector Proteins to the Replicative Vacuole. PLoS Pathog. *2*, e46. 10.1371/journal.ppat.0020046.

27. Schoebel, S., Blankenfeldt, W., Goody, R.S., and Itzen, A. (2010). High-affinity binding of phosphatidylinositol 4-phosphate by Legionella pneumophila DrrA. EMBO Rep. *11*, 598–604. 10.1038/embor.2010.97.

28. Clemens, D.L., Lee, B.-Y., and Horwitz, M.A. (2000). Deviant Expression of Rab5 on Phagosomes Containing the Intracellular Pathogens Mycobacterium tuberculosis and Legionella pneumophila Is Associated with Altered Phagosomal Fate. Infect. Immun. *68*, 2671–2684. 10.1128/iai.68.5.2671-2684.2000.

29. Clemens, D.L., Lee, B.-Y., and Horwitz, M.A. (2000). Mycobacterium tuberculosis and Legionella pneumophila Phagosomes Exhibit Arrested Maturation despite Acquisition of Rab7. Infect. Immun. *68*, 5154–5166. 10.1128/iai.68.9.5154-5166.2000.

30. Hoffmann, C., Finsel, I., Otto, A., Pfaffinger, G., Rothmeier, E., Hecker, M., Becher, D., and Hilbi, H. (2014). Functional analysis of novel Rab GTPases identified in the proteome of purified Legionella-containing vacuoles from macrophages. Cell. Microbiol. *16*, 1034–1052. 10.1111/cmi.12256.

31. Gaspar, A.H., and Machner, M.P. (2014). VipD is a Rab5-activated phospholipase A1 that protects Legionella pneumophila from endosomal fusion. Proc. Natl. Acad. Sci. *111*, 4560–4565. 10.1073/pnas.1316376111.

32. Simonsen, A., Lippe, R., Christoforidis, S., Gaullier, J.-M., Brech, A., Callaghan, J., Toh, B.-H., Murphy, C., Zerial, M., and Stenmark, H. (1998). EEA1 links PI(3)K function to Rab5 regulation of endosome fusion. Nature *394*, 494–498. 10.1038/28879.

33. Xu, H., and Wickner, W. (2010). Phosphoinositides Function Asymmetrically for Membrane Fusion, Promoting Tethering and 3Q-SNARE Subcomplex Assembly. J. Biol. Chem. *285*, 39359–39365. 10.1074/jbc.m110.183111.

34. Joshi, A.D., Sturgill-Koszycki, S., and Swanson, M.S. (2001). Evidence that Dot-dependent and -independent factors isolate the Legionella pneumophila phagosome from the endocytic network in mouse macrophages. Cell. Microbiol. *3*, 99–114. 10.1046/j.1462-5822.2001.00093.x.

35. Sohn, Y.-S., Shin, H.-C., Park, W.S., Ge, J., Kim, C.-H., Lee, B.L., Heo, W.D., Jung, J.U., Rigden, D.J., and Oh, B.-H. (2015). Lpg0393 of Legionella pneumophila Is a Guanine-Nucleotide Exchange Factor for Rab5, Rab21 and Rab22. PLoS ONE *10*, e0118683. 10.1371/journal.pone.0118683.

36. Coers, J., Monahan, C., and Roy, C.R. (1999). Modulation of phagosome biogenesis by Legionella pneumophila creates an organelle permissive for intracellular growth. Nat. Cell Biol. *1*, 451–453. 10.1038/15687.

37. Kang, Y.-S., and Kirby, J.E. (2017). Promotion and Rescue of Intracellular Brucella neotomae Replication during Coinfection with Legionella pneumophila. Infect. Immun. *85*. 10.1128/iai.00991-16.

38. McClellan, A.J., Laugesen, S.H., and Ellgaard, L. (2019). Cellular functions and molecular mechanisms of non-lysine ubiquitination. Open Biol. *9*, 190147. 10.1098/rsob.190147.

39. Komander, D., and Rape, M. (2012). The Ubiquitin Code. Annu. Rev. Biochem. *81*, 203–229. 10.1146/annurev-biochem-060310-170328.

40. Piper, R.C., Dikic, I., and Lukacs, G.L. (2014). Ubiquitin-Dependent Sorting in Endocytosis. Cold Spring Harb. Perspect. Biol. *6*, a016808. 10.1101/cshperspect.a016808.

41. Wan, M., Wang, X., Huang, C., Xu, D., Wang, Z., Zhou, Y., and Zhu, Y. (2019). A bacterial effector deubiquitinase specifically hydrolyses linear ubiquitin chains to inhibit host inflammatory signalling. Nat. Microbiol. *4*, 1282–1293. 10.1038/s41564-019-0454-1.

42. Cemma, M., and Brumell, J.H. (2012). Interactions of Pathogenic Bacteria with Autophagy Systems. Curr. Biol. *22*, R540–R545. 10.1016/j.cub.2012.06.001.

43. Luo, J., Wang, L., Song, L., and Luo, Z.-Q. (2021). Exploitation of the Host Ubiquitin System: Means by Legionella pneumophila. Front. Microbiol. *12*, 790442. 10.3389/fmicb.2021.790442.

44. Luo, Z.-Q., and Isberg, R.R. (2004). Multiple substrates of the Legionella pneumophila Dot/Icm system identified by interbacterial protein transfer. Proc. Natl. Acad. Sci. *101*, 841–846. 10.1073/pnas.0304916101.

45. Ragaz, C., Pietsch, H., Urwyler, S., Tiaden, A., Weber, S.S., and Hilbi, H. (2008). The Legionella pneumophila phosphatidylinositol-4 phosphate-binding type IV substrate SidC recruits endoplasmic reticulum vesicles to a replication-permissive vacuole. Cell. Microbiol. *10*, 2416–2433. 10.1111/j.1462-5822.2008.01219.x.

46. Hsu, F., Luo, X., Qiu, J., Teng, Y.-B., Jin, J., Smolka, M.B., Luo, Z.-Q., and Mao, Y. (2014). The Legionella effector SidC defines a unique family of ubiquitin ligases important for bacterial phagosomal remodeling. Proc. Natl. Acad. Sci. *111*, 10538–10543. 10.1073/pnas.1402605111.

47. Horenkamp, F.A., Mukherjee, S., Alix, E., Schauder, C.M., Hubber, A.M., Roy, C.R., and Reinisch, K.M. (2014). Legionella pneumophila Subversion of Host Vesicular Transport by SidC Effector Proteins. Traffic *15*, 488–499. 10.1111/tra.12158.

48. Jeng, E.E., Bhadkamkar, V., Ibe, N.U., Gause, H., Jiang, L., Chan, J., Jian, R., Jimenez-Morales, D., Stevenson, E., Krogan, N.J., et al. (2019). Systematic Identification of Host Cell Regulators of Legionella pneumophila Pathogenesis Using a Genome-wide CRISPR Screen. Cell Host Microbe *26*, 551-563.e6. 10.1016/j.chom.2019.08.017.

49. Bhogaraju, S., Kalayil, S., Liu, Y., Bonn, F., Colby, T., Matic, I., and Dikic, I. (2016). Phosphoribosylation of Ubiquitin Promotes Serine Ubiquitination and Impairs Conventional Ubiquitination. Cell *167*, 1636-1649.e13. 10.1016/j.cell.2016.11.019.

50. Qiu, J., Sheedlo, M.J., Yu, K., Tan, Y., Nakayasu, E.S., Das, C., Liu, X., and Luo, Z.-Q. (2016). Ubiquitination independent of E1 and E2 enzymes by bacterial effectors. Nature *533*, 120–124. 10.1038/nature17657.

51. 10.7554/elife.58114.

52. Ong, S.Y., Schuelein, R., Wibawa, R.R., Thomas, D.W., Handoko, Y., Freytag, S., Bahlo, M., Simpson, K.J., and Hartland, E.L. (2021). Genome-wide genetic screen identifies host ubiquitination as important for Legionella pneumophila Dot/Icm effector translocation. Cell. Microbiol. *23*, e13368. 10.1111/cmi.13368.

53. Li, X., Anderson, D.E., Chang, Y.-Y., Jarnik, M., and Machner, M.P. (2022). VpdC is a ubiquitin-activated phospholipase effector that regulates Legionella vacuole expansion during infection. Proc. Natl. Acad. Sci. *119*, e2209149119. 10.1073/pnas.2209149119.

54. Ivanov, S.S., and Roy, C.R. (2009). Modulation of ubiquitin dynamics and suppression of DALIS formation by the Legionella pneumophila Dot/Icm system. Cell. Microbiol. *11*, 261–278. 10.1111/j.1462-5822.2008.01251.x.

55. Anand, I., Choi, W., and Isberg, R.R. (2020). The vacuole guard hypothesis: how intravacuolar pathogens fight to maintain the integrity of their beloved home. Curr. Opin. Microbiol. *54*, 51–58. 10.1016/j.mib.2020.01.008.

56. Beuzón, C.R., Méresse, S., Unsworth, K.E., Ruíz-Albert, J., Garvis, S., Waterman, S.R., Ryder, T.A., Boucrot, E., and Holden, D.W. (2000). Salmonella maintains the integrity of its intracellular vacuole through the action of SifA. EMBO J. *19*, 3235–3249. 10.1093/emboj/19.13.3235.

57. Choi, W.Y., Kim, S., Aurass, P., Huo, W., Creasey, E.A., Edwards, M., Lowe, M., and Isberg, R.R. (2021). SdhA blocks disruption of the Legionella-containing vacuole by hijacking the OCRL phosphatase. Cell Rep. *37*, 109894. 10.1016/j.celrep.2021.109894.

58. Laguna, R.K., Creasey, E.A., Li, Z., Valtz, N., and Isberg, R.R. (2006). A Legionella pneumophila-translocated substrate that is required for growth within macrophages and protection from host cell death. Proc. Natl. Acad. Sci. *103*, 18745–18750. 10.1073/pnas.0609012103.

59. Kim, S., and Isberg, R.R. (2023). The Sde phosphoribosyl–linked ubiquitin transferases protect the Legionella pneumophila vacuole from degradation by the host. Proc. Natl. Acad. Sci. *120*, e2303942120. 10.1073/pnas.2303942120.

60. Isberg, R., Kotewicz, K., Zheng, M., Kim, S., and Tai, A. (2023). Sde Proteins Coordinate Ubiquitin Utilization and Phosphoribosylation to Promote Establishment and Maintenance of the Legionella Replication Vacuole. Res. Sq., rs.3.rs-3269310. 10.21203/rs.3.rs-3269310/v1.

61. Shin, H.-W., Hayashi, M., Christoforidis, S., Lacas-Gervais, S., Hoepfner, S., Wenk, M.R., Modregger, J., Uttenweiler-Joseph, S., Wilm, M., Nystuen, A., et al. (2005). An enzymatic cascade of Rab5 effectors regulates phosphoinositide turnover in the endocytic pathway. J. Cell Biol. *170*, 607–618. 10.1083/jcb.200505128.

62. Mishra, A., Eathiraj, S., Corvera, S., and Lambright, D.G. (2010). Structural basis for Rab GTPase recognition and endosome tethering by the C2H2 zinc finger of Early Endosomal Autoantigen 1 (EEA1). Proc. Natl. Acad. Sci. *107*, 10866–10871. 10.1073/pnas.1000843107.

63. Dong, N., Niu, M., Hu, L., Yao, Q., Zhou, R., and Shao, F. (2016). Modulation of membrane phosphoinositide dynamics by the phosphatidylinositide 4-kinase activity of the Legionella LepB effector. Nat. Microbiol. *2*, 16236. 10.1038/nmicrobiol.2016.236.

64. Mukherjee, S., Liu, X., Arasaki, K., McDonough, J., Galán, J.E., and Roy, C.R. (2011). Modulation of Rab GTPase function by a protein phosphocholine transferase. Nature *477*, 103–106. 10.1038/nature10335.

65. Treacy-Abarca, S., and Mukherjee, S. (2015). Legionella suppresses the host unfolded protein response via multiple mechanisms. Nat. Commun. *6*, 7887. 10.1038/ncomms8887.

66. Black, M.H., Osinski, A., Gradowski, M., Servage, K.A., Pawłowski, K., Tomchick, D.R., and Tagliabracci, V.S. (2019). Bacterial pseudokinase catalyzes protein polyglutamylation to inhibit the SidE-family ubiquitin ligases. Science *364*, 787–792. 10.1126/science.aaw7446.

67. Kim, W., Bennett, E.J., Huttlin, E.L., Guo, A., Li, J., Possemato, A., Sowa, M.E., Rad, R., Rush, J., Comb, M.J., et al. (2011). Systematic and Quantitative Assessment of the Ubiquitin-Modified Proteome. Mol. Cell *44*, 325–340. 10.1016/j.molcel.2011.08.025.

68. Steinbach, A., Bhadkamkar, V., Jimenez-Morales, D., Stevenson, E., Jang, G.M., Krogan, N.J., Swaney, D.L., and Mukherjee, S. (2024). Cross-family small GTPase ubiquitination by the intracellular pathogen Legionella pneumophila. Mol. Biol. Cell *35*, ar27. 10.1091/mbc.e23-06-0260.

69. Gomes, A.Q., Ali, B.R., Ramalho, J.S., Godfrey, R.F., Barral, D.C., Hume, A.N., and Seabra, M.C. (2003). Membrane Targeting of Rab GTPases Is Influenced by the Prenylation Motif. Mol. Biol. Cell *14*, 1882–1899. 10.1091/mbc.e02-10-0639.

70. Shin, D., Mukherjee, R., Liu, Y., Gonzalez, A., Bonn, F., Liu, Y., Rogov, V.V., Heinz, M., Stolz, A., Hummer, G., et al. (2020). Regulation of Phosphoribosyl-Linked Serine Ubiquitination by Deubiquitinases DupA and DupB. Mol. Cell *77*, 164-179.e6. 10.1016/j.molcel.2019.10.019.

71. Anand, I.S., Choi, W., and Isberg, R.R. (2020). Components of the endocytic and recycling trafficking pathways interfere with the integrity of the Legionella-containing vacuole. Cell. Microbiol. *22*, e13151. 10.1111/cmi.13151.

72. Kawabata, M., Matsuo, H., Koito, T., Murata, M., Kubori, T., Nagai, H., Tagaya, M., and Arasaki, K. (2021). Legionella hijacks the host Golgi-to-ER retrograde pathway for the association of Legionella-containing vacuole with the ER. PLoS Pathog. *17*, e1009437. 10.1371/journal.ppat.1009437.

73. Wasilko, D.J., Huang, Q., and Mao, Y. (2018). Insights into the ubiquitin transfer cascade catalyzed by the Legionella effector SidC. eLife *7*, e36154. 10.7554/elife.36154.

74. Luo, X., Wasilko, D.J., Liu, Y., Sun, J., Wu, X., Luo, Z.-Q., and Mao, Y. (2015). Structure of the Legionella Virulence Factor, SidC Reveals a Unique PI(4)P-Specific Binding Domain Essential for Its Targeting to the Bacterial Phagosome. PLoS Pathog. *11*, e1004965. 10.1371/journal.ppat.1004965.

75. Shin, D., Na, W., Lee, J.-H., Kim, G., Baek, J., Park, S.H., Choi, C.Y., and Lee, S. (2017). Site-specific monoubiquitination downregulates Rab5 by disrupting effector binding and guanine nucleotide conversion. eLife *6*, e29154. 10.7554/elife.29154.

76. Horiuchi, H., Lippé, R., McBride, H.M., Rubino, M., Woodman, P., Stenmark, H., Rybin, V., Wilm, M., Ashman, K., Mann, M., et al. (1997). A Novel Rab5 GDP/GTP Exchange Factor Complexed to Rabaptin-5 Links Nucleotide Exchange to Effector Recruitment and Function. Cell *90*, 1149–1159. 10.1016/s0092-8674(00)80380-3.

77. Stenmark, H., Parton, R.G., Steele-Mortimer, O., Lütcke, A., Gruenberg, J., and Zerial, M. (1994). Inhibition of rab5 GTPase activity stimulates membrane fusion in endocytosis. EMBO J. *13*, 1287–1296. 10.1002/j.1460-2075.1994.tb06381.x.

78. Lauer, J., Segeletz, S., Cezanne, A., Guaitoli, G., Raimondi, F., Gentzel, M., Alva, V., Habeck, M., Kalaidzidis, Y., Ueffing, M., et al. (2019). Auto-regulation of Rab5 GEF activity in Rabex5 by allosteric structural changes, catalytic core dynamics and ubiquitin binding. eLife *8*, e46302. 10.7554/elife.46302.

79. Bucci, C., Parton, R.G., Mather, I.H., Stunnenberg, H., Simons, K., Hoflack, B., and Zerial, M. (1992). The small GTPase rab5 functions as a regulatory factor in the early endocytic pathway. Cell *70*, 715–728. 10.1016/0092-8674(92)90306-w.

80. Goldenthal, K.L., Hedman, K., Chen, J.W., August, J.T., and Willingham, M.C. (1985). Postfixation detergent treatment for immunofluorescence suppresses localization of some integral membrane proteins. J. Histochem. Cytochem. : Off. J. Histochem. Soc. *33*, 813–820. 10.1177/33.8.3894499.

81. Dorer, M.S., Kirton, D., Bader, J.S., and Isberg, R.R. (2006). RNA Interference Analysis of Legionella in Drosophila Cells: Exploitation of Early Secretory Apparatus Dynamics. PLoS Pathog. *2*, e34. 10.1371/journal.ppat.0020034.

82. Kubori, T., Shinzawa, N., Kanuka, H., and Nagai, H. (2010). Legionella Metaeffector Exploits Host Proteasome to Temporally Regulate Cognate Effector. PLoS Pathog. *6*, e1001216. 10.1371/journal.ppat.1001216.

83. Clague, M.J., Heride, C., and Urbé, S. (2015). The demographics of the ubiquitin system. Trends Cell Biol. *25*, 417–426. 10.1016/j.tcb.2015.03.002.

84. Medvar, B., Raghuram, V., Pisitkun, T., Sarkar, A., and Knepper, M.A. (2016). Comprehensive database of human E3 ubiquitin ligases: application to aquaporin-2 regulation. Physiol. Genom. *48*, 502–512. 10.1152/physiolgenomics.00031.2016.

85. Allton, K., Jain, A.K., Herz, H.-M., Tsai, W.-W., Jung, S.Y., Qin, J., Bergmann, A., Johnson, R.L., and Barton, M.C. (2009). Trim24 targets endogenous p53 for degradation. Proc. Natl. Acad. Sci. *106*, 11612–11616. 10.1073/pnas.0813177106.

86. Jain, A.K., Allton, K., Duncan, A.D., and Barton, M.C. (2014). TRIM24 Is a p53-Induced E3-Ubiquitin Ligase That Undergoes ATM-Mediated Phosphorylation and Autodegradation during DNA Damage. Mol. Cell. Biol. *34*, 2695–2709. 10.1128/mcb.01705-12.

87. Sulpizio, A., Minelli, M.E., Wan, M., Burrowes, P.D., Wu, X., Sanford, E.J., Shin, J.-H., Williams, B.C., Goldberg, M.L., Smolka, M.B., et al. (2019). Protein polyglutamylation catalyzed by the bacterial calmodulin-dependent pseudokinase SidJ. eLife *8*, e51162. 10.7554/elife.51162.

88. Jeong, K.C., Sexton, J.A., and Vogel, J.P. (2015). Spatiotemporal Regulation of a Legionella pneumophila T4SS Substrate by the Metaeffector SidJ. PLoS Pathog. *11*, e1004695. 10.1371/journal.ppat.1004695.

89. Joseph, A.M., Pohl, A.E., Ball, T.J., Abram, T.G., Johnson, D.K., Geisbrecht, B.V., and Shames, S.R. (2020). The Legionella pneumophila Metaeffector Lpg2505 (MesI) Regulates SidI-Mediated Translation Inhibition and Novel Glycosyl Hydrolase Activity. Infect. Immun. *88*. 10.1128/iai.00853-19.

90. Berger, K.H., and Isberg, R.R. (1993). Two distinct defects in intracellular growth complemented by a single genetic locus in Legionella pneumophila. Mol. Microbiol. *7*, 7–19. 10.1111/j.1365-2958.1993.tb01092.x.

91. Berger, K.H., Merriam, J.J., and Isberg, R.R. (1994). Altered intracellular targeting properties associated with mutations in the Legionella pneumophila dotA gene. Mol. Microbiol. *14*, 809–822. 10.1111/j.1365-2958.1994.tb01317.x.

92. Cox, J., Hein, M.Y., Luber, C.A., Paron, I., Nagaraj, N., and Mann, M. (2014). Accurate Proteome-wide Label-free Quantification by Delayed Normalization and Maximal Peptide Ratio Extraction, Termed MaxLFQ*. Mol. Cell. Proteom. *13*, 2513–2526. 10.1074/mcp.m113.031591.

93. Choi, M., Chang, C.-Y., Clough, T., Broudy, D., Killeen, T., MacLean, B., and Vitek, O. (2014). MSstats: an R package for statistical analysis of quantitative mass spectrometry-based proteomic experiments. Bioinformatics *30*, 2524–2526. 10.1093/bioinformatics/btu305.

94. Webb-Robertson, B.-J.M., Wiberg, H.K., Matzke, M.M., Brown, J.N., Wang, J., McDermott, J.E., Smith, R.D., Rodland, K.D., Metz, T.O., Pounds, J.G., et al. (2015). Review, Evaluation, and Discussion of the Challenges of Missing Value Imputation for Mass Spectrometry-Based Label-Free Global Proteomics. J. Proteome Res. *14*, 1993–2001. 10.1021/pr501138h.

95. Vizcaíno, J.A., Csordas, A., del-Toro, N., Dianes, J.A., Griss, J., Lavidas, I., Mayer, G., Perez-Riverol, Y., Reisinger, F., Ternent, T., et al. (2016). 2016 update of the PRIDE database and its related tools. Nucleic Acids Res. *44*, D447–D456. 10.1093/nar/gkv1145.

96. Hulsen, T. (2022). DeepVenn -- a web application for the creation of area-proportional Venn diagrams using the deep learning framework Tensorflow.js. arXiv. 10.48550/arxiv.2210.04597.

97. Waterhouse, A.M., Procter, J.B., Martin, D.M.A., Clamp, M., and Barton, G.J. (2009). Jalview Version 2—a multiple sequence alignment editor and analysis workbench. Bioinformatics *25*, 1189–1191. 10.1093/bioinformatics/btp033.

98. Schindelin, J., Arganda-Carreras, I., Frise, E., Kaynig, V., Longair, M., Pietzsch, T., Preibisch, S., Rueden, C., Saalfeld, S., Schmid, B., et al. (2012). Fiji: an open-source platform for biological-image analysis. Nat. Methods *9*, 676–682. 10.1038/nmeth.2019.

99. Stirling, D.R., Swain-Bowden, M.J., Lucas, A.M., Carpenter, A.E., Cimini, B.A., and Goodman, A. (2021). CellProfiler 4: improvements in speed, utility and usability. BMC Bioinform. *22*, 433. 10.1186/s12859-021-04344-9.

Publishing Agreement

It is the policy of the University to encourage open access and broad distribution of all theses, dissertations, and manuscripts. The Graduate Division will facilitate the distribution of UCSF theses, dissertations, and manuscripts to the UCSF Library for open access and distribution. UCSF will make such theses, dissertations, and manuscripts accessible to the public and will take reasonable steps to preserve these works in perpetuity.

I hereby grant the non-exclusive, perpetual right to The Regents of the University of California to reproduce, publicly display, distribute, preserve, and publish copies of my thesis, dissertation, or manuscript in any form or media, now existing or later derived, including access online for teaching, research, and public service purposes.

DocuSigned by:

_____

A1BBDE4DCCE8490...   Author Signature

5/28/2024
_____

Date

71